SOA Research INSTITUTE

Potential Impacts of Climate Change on U.S. Inland Flood Risk by Mid Century

Catastrophe and Climate

November 2021

Potential Impacts of Climate Change on U.S. Inland Flood Risk by Mid Century

AUTHORS Peter Sousounis, PhD
Vice President/Director of Climate Change Research
AIR Worldwide
Boston, MA 02111

Alastair Clarke, PhD
Senior Research Associate
AIR Worldwide
London, UK

Doug Fullam
Director, Life and Health Modeling
AIR Worldwide
Boston, MA 02111

SPONSOR Catastrophe and Climate Strategic Research Program Steering Committee

CONTENTS

Potential Impacts of Climate Change on U.S. Inland Flood Risk by Mid Century

Executive Summary

Impacts to U.S. property losses from future climate change on U.S. inland flood risk by 2050 under an assumed Representative Concentration Pathway (RCP) 8.5 are evaluated using the AIR Inland Flood Model for the United States, the AIR Hurricane Model for the United States, and downscaled (i.e., increased horizontal resolution from what is otherwise available) output from future climate runs with General Circulation Models (GCMs). Understanding the potential impacts to return period (RP) event, or occurrence, losses rather than to annual aggregate losses, i.e., from all flood loss-causing events in a single year, is the primary focus. The AIR Inland Flood Model captures the current flood risk for the contiguous U.S. from all precipitation sources except for hurricanes and the AIR Hurricane Model does the same but quantifies the inland flood risk from hurricane-induced precipitation. Both models contain 10,000 years' worth of flood events that could occur in today's climate. The RCP 8.5 greenhouse gas concentration-based climate scenario is a fossil-fueled development scenario and one that society have been following since 2005. The period through 2050 is relevant for practice of Society of Actuaries members.

Based on simple thermodynamics, a warming atmosphere will allow for more water vapor and all else being equal this should translate to an increase in precipitation – about seven percent per degree Celsius according to the Clausius-Clapeyron relationship. But climate change will also likely yield changes in large scale atmospheric circulation patterns that may change where, when, and how often that increased precipitation may fall. Other factors such as evaporation rate, which is based on wind speed, temperature, and humidity will affect the result. An overview of the complexity of floods is provided to demonstrate that floods involve more than just heavy precipitation, especially ones from overflowing long and large rivers. A demonstration that heavy precipitation is changing across the U.S. – because of climate change - is also provided. Results from some relevant recent studies are provided to demonstrate what is generally expected, what is known, and what is not known about climate change impacts to flood.

The basic approach for this study involves using available downscaled output from five different GCMs as part of the Coupled Model Intercomparison Project Phase 5 (CMIP5) to evaluate how on-plain (riverine) and off-plain (urban) flood risk may change[1]. On-plain annual occurrence maps for nine different return periods at 1 km resolution are sourced from Aqueduct Floods. Three extra return periods are created, and the maps are aggregated to the county-level. Daily precipitation at 4 km resolution, downscaled from the same five GCMs, is used to obtain county-level annual occurrence maps for twelve return periods. These maps are evaluated to understand how heavy precipitation events that cause off-plain flooding may change in the future. The RP hazard views from the GCMs for the current climate are combined with RP loss information from the AIR Models to create county-specific on- and off-plain damage functions. The damage functions are then used in conjunction with future flood depths and maximum daily precipitation to determine relative changes to annual occurrence losses at twelve return periods. Losses across the U.S. are evaluated using information from the AIR U.S. Industry Exposure Database, which contains

[1] Flash flooding is not addressed as a separate type of flooding because it manifests as either on-plain or off-plain flooding.

information on all insurable properties in the U.S., including replacement value. Losses also include a time-element factor to account for business being interrupted because of repairs from flood damage.

Results from a mean GCM based view suggest that on-plain flooding will increase along parts of the Missouri and Mississippi River Basins as well as portions of the Appalachian Mountains. Other areas will likely see decreases in on-plain flooding such as northern California and portions of the Pacific Northwest, portions of the southern Rockies, the northern Great Plains, and southern Great Plains. Results for off-plain flooding, which is more closely tied to occurrences of heavy precipitation, suggest that increases will occur across much of California and portions of the Pacific Northwest, the Gulf Coast States except for Florida, a ribbon-like area through the Midwest, and the northern New England states. Because changes in loss are directly related to the changes in on- and off-plain flood depths that are calculated for the future, the changes in the return period on- and off-plain flood losses mirror the changes in the hazard, modulated considerably by exposure concentration and value.

Annual occurrence losses (AOLs) at the county level are computed in addition to RP losses by integrating the information at the available return periods. The spatial distributions of AOLs for on- and off-plain flooding are similar to those for the return periods but yield broader regions where flood losses may increase (or decrease) than do the individual RP views, because of the integration. Particularly noteworthy are the increases in AOL over the northern intermountain region (Montana), most of Nevada (because of the many small rivers in that state, Southwest Texas along the Rio Grande River, broader areas of the Missouri River and Mississippi River Basins, the Wabash River Basin straddling the border between Illinois and Indiana, and portions of the Appalachians and southern New England states. The county-level AOLs for off-plain flood loss show increases over many counties west of the Appalachians, with the exception of the intermountain region. Exceptions in that broad region include small decreases across northern Texas and Missouri and central Michigan. East of the Appalachians increases in off-plain county-level AOLs occur in northern Florida, coastal Southeastern U.S. states, Long Island, and coastal New England states.

Further clarity is obtained by considering where the county-level AOLs for on- and off-plain flooding correlate in terms of the directional change in loss e.g., both positive, or both negative. Increases in both occur over the coastal Pacific Northwest, Nevada, a broad swath extending southeastward from Montana to the central Midwest, Southwest Texas and southern New Mexico, the southern Mississippi, the southern Appalachians, and coastal mid-Atlantic and New England states.

Further aggregation was accomplished to the state level using approximate relationships that were developed to understand how actual state-level AOLs for the current climate relate to estimates based on assumptions of zero and perfect inter-county correlation. The degree of correlation obtained for each county was then applied to the future climate results to obtain changes in state-level AOLs. The results are consistent with those at the county level but greatly influenced by where AOL changes at the county level are greatest. Lastly, a national view was created using a similar technique for aggregating county-level to state-level. On a national scale, the AOLs for on- and off-plain flooding are approximately -6% and +49% respectively. Because dollar values from each of these are comparable, the net change at the national level would be an annual increase.

Results from the mean GCM view are placed into context with an evaluation of results from the five GCMs used. Results for changes in hazard and hence changes in loss show considerable spread although a consensus map does show that the results obtained from the mean GCM view are the result of a majority (i.e., three or more of the five) of models agreeing in areas where increases and decreases may occur. The 5-95% confidence interval for the national view for changes in on-plain AOL ranges from -47% to +69% and the same confidence interval for changes in off-plain range from -29% to +163%. These considerable uncertainty ranges demonstrate that it is difficult to be certain how climate change will affect future U.S. inland flood risk. The uncertainty stemming from different GCM outputs is magnified in the downscaling process, but this process is necessary to investigate extreme events like floods.

A comparison of results from this study to those from the companion study on how climate change may impact U.S. Wildfire risk shows that much of the domain evaluated for U.S. Wildfire (13 western states) would experience increased losses from wildfire and either on- or off- plain flooding by mid-century. However, using a combined peril AOL view (i.e., summing the AOLs for all three risks even though they are not part of the same event) shows that most areas would experience a net annual increase less than 25% above that for the current climate.

The results of this study yield useful information about how inland flood risk and loss may change across the U.S. in the future because of climate change under the assumptions of a particular RCP scenario, which is a subset of climate projection information from GCMs. No changes in resiliency measures (e.g., more levees, better drainage), or industry exposure, or building codes were considered in this study. Future studies are recommended to address some, or all, of the limitations noted above. By providing estimates of the cost of not mitigating greenhouse gas emissions and not adapting to changing flood risk, this study can be used to estimate the savings made by transitioning to a greener economy and improving urban drainage capacities and flood defenses in specific areas of the U.S.

Section 1: Introduction

Frequency and intensity of flooding have increased during the last several decades across many parts of the U.S. Hurricane Harvey in 2017 demonstrated that single-event floods can cause big losses that dominate even those from wind in a hurricane. Several studies indicate a connection to climate variability and change and a big concern therefore is that as climate change continues the flood risk will worsen. This report provides results from a recently conducted study using the AIR Inland Flood Model for the United States and available climate and climate change information to estimate how climate change may influence single event return period losses to U.S. property by mid-century. The focus is on inland flooding from precipitation, as opposed to coastal flooding from storm surge and sea level rise. The AIR Model and current climate information are used to create county-specific flood damage functions and the future climate information is then used to determine how return period losses will change. Additionally, because flood in the U.S. is a risk that is insured primarily by the Federal Government for residential property, the losses we consider in this study are from an insurable standpoint rather than an insured standpoint. The latter refers to property covered under private insurance. The former refers to any structure considered to be insurable from a structural and use standpoint including buildings for residence, commerce, and industry and includes mobile homes, automobiles, and contents within structures, whether it is or is not covered under any insurance policy.

The climate change scenario used for this study is defined by a mid-century (2050) time horizon under an assumed RCP 8.5 scenario. The RCP 8.5 greenhouse gas concentration scenario was chosen to explore the consequences of a world with limited action taken to address climate change. Although Hausfather and Peters (2020) suggested that greenhouse gas concentrations already departed to the low side from RCP 8.5, Schwalm *et al.* (2020) showed that RCP 8.5 is in close agreement with historic emissions and that RCP 8.5 is the best match of the four available RCPs "out to midcentury under current and stated [national energy] policies." Even though greenhouse gas emission rates declined modestly because of the COVID-19 pandemic, they may recover quickly post-pandemic. On balance, RCP 8.5 remains a plausible upper bound and a useful analytical reference point.

As our climate continues to warm, there are even more concerns about how increasing temperatures from greenhouse gasses will influence rainfall patterns. But rainfall is only one component of the flood phenomenon. Floods are complex and can occur in different ways and in different places. To appreciate the complex nature of understanding how climate change may influence floods, we first take a brief look at the physics of floods.

1.1 THE PHYSICS OF FLOODS

How much water falls in how much time is an important consideration for flood. But it is not the only one. What happens to the water when it reaches the ground and in fact the complete life cycle of a water drop (or snowflake or any type of precipitation for that matter) depends on the characteristics of the surface and below, the weather conditions possibly over the subsequent 2-3 weeks sometimes even thousands of river network miles away, and any natural or technological measures of resilience and practices for managing them. We provide an overview of the salient features for the three main components below.

1.1.1 PRECIPITATION AND EVAPORATION

Precipitation comes from almost every weather phenomenon from hurricanes, to winter storms, to fronts, to isolated convective storms. To understand the evolution of a flood, it is important to account for precipitation from all these systems as well as to account for sources of water from weather systems like melting snowfall from systems earlier in the (hydrological) year. The source of the precipitation is water that evaporates from water bodies like oceans, lakes, rivers but even from puddles on streets and pavements, and even from moisture from plants, and animals (including humans), and the ground itself. The rate of evaporation depends on temperature, the amount of moisture already in the atmosphere, wind speed, and more.

The timing of precipitation can be important for floods. Even a large and very wet weather system that produces a one-inch rainfall across a widespread (e.g., multi-state) region may not cause a flood if antecedent soil moisture conditions are dry and river levels in the area (watershed) are low. However, several such events over the course of a season can ultimately cause significant flooding adjacent to rivers and streams.

1.1.2 HYDROLOGY AND GROUNDFLOW

Once precipitation hits the ground, the regional topography, predominant soil type, and geology are important factors in determining how much water will infiltrate into the ground surface and how much will flow over land or through small streams. Infiltration capacity depends on the unique combination of soil type and the thickness and porosity of the underlying water-bearing rock formation, or aquifer. Aquifers serve as large reservoirs, storing groundwater and releasing it over long periods of time after a storm, thus reducing the variability of river flow and preventing rivers from flooding.

Topography (land slope) plays a major role in how precipitation and excess runoff flows over land. When snow in higher elevations melts, the runoff, which may be intensified by additional rainfall, can flow downslope and swell rivers downstream. Floods accumulate in low-lying areas and the relatively flat land in the floodplains that surround large rivers can be highly flood prone.

Igneous rocks (e.g., basalt and granite) have a very low infiltration capacity. In contrast, marine sedimentary rocks (e.g., limestone) have a high infiltration capacity, as they are often rich in calcium carbonate, a mineral conducive to dissolution. Acidic precipitation, moving through cracks, dissolves the surrounding rock, and can lead to the formation of karst—a network of caverns, and subterranean streams. Karst regions can have tremendous infiltration capacities. Rivers may spring from, or disappear into, the rock formation. Other sedimentary rocks (e.g., sandstone and shale) consist of lithified sand and clay. The infiltration capacity of sandstone or shale is usually low unless heavily fractured.

Land cover may significantly affect runoff. In forested areas, tree roots create channels deep into the soil, down to groundwater, increasing infiltration and reducing surface runoff. In urban areas, the high percentage of paved areas may increase runoff significantly.

Finally, debris in the water can also act to impede flow. Uprooted trees, boulders, even ice jams during spring thaw can lead to or exacerbate floods.

1.1.1 FLOOD DEFENCES AND FLOOD MANAGMENT

Dams exist to hold back water to maintain a water supply for various needs and activities. Levees are built along adjacent riverbanks in flood prone areas to mitigate risk. Design specs are usually based on historical experience and typically built to withstand what is expected to be a 100-year flood. Cost is factored into the design spec including materials. Sewers and cisterns are similarly designed and built based on knowledge of past history.

1.2 FLOOD TYPES

Inland floods that occur near rivers can be among the longest lasting, largest in area, deepest in terms of flood water depth, and hence the most catastrophic. These floods are referred to as fluvial and typically impact the flood plain at various return period heights and areas straddling rivers. This type is referred to as on-plain flooding. Flooding can also occur in areas far away from rivers, from sudden heavy precipitation that can overwhelm existing sewer and other drainage systems. These pluvial, or off-plain floods can occur almost anywhere and at any time almost independent of antecedent or surface conditions. In the presence of steep terrain flash flooding can occur as a type of off-plain or on-plain flooding. We look in some detail at the distinction between the two. Both are important. Both contribute significantly to property loss as well as to loss of life.

1.2.1 ON-PLAIN FLOODING

Overbank flooding of rivers and streams – the increase in volume of water within a river channel and the overflow of water from the channel onto the adjacent floodplain – represents the classic flooding event that most people associate with the term "flood." In fact, this is also the most common type of flood event. Hundreds of riverine floods, great and small, occur annually in the United States. Riverine floodplains range from narrow, confined channels (as in steep river valleys in hilly and mountainous areas) to wide, flat areas (as in much of the Midwest and in many coastal areas). In the steep narrow valleys, flooding usually occurs quickly and is of short duration, but is likely to be rapid and deep. In relatively flat floodplains, areas may remain inundated for days or even weeks, but floodwaters are typically slow-moving and shallow. Along major rivers with very large drainage basins, the timing and elevations of flood peaks can be predicted far in advance and with considerable accuracy. In very small basins, flooding may be more difficult to predict to provide useful warning time. Generally, the smaller the drainage basin, the more difficult it is to forecast the flood. Flooding in large rivers usually results from large-scale weather systems generating prolonged rainfall over wide areas. These same weather systems may cause flooding in hundreds of smaller basins that drain into the major river system. The streams and small rivers are also susceptible to flooding from more localized weather systems that cause intense rainfall over only a small area. In parts of the northern and western United States, annual spring floods result from spring snowmelt and the extent of flooding is dependent upon winter snowpack and spring weather patterns. Several high-risk or unusual types of riverine flooding are described in the following sections. There is often no sharp distinction between flash floods, flooding due to structural failure or overtopping, flooding on alluvial fans, and the other types of high-risk flooding described. There is much overlap among these types of floods that tend to represent different characteristics of the entire range of riverine flooding. However, the following categories are widely recognized and helpful in considering not only the range of flood risk but also appropriate responses to the risk (FEMA 2007).

For most management purposes in the United States today, floodplains are defined as the lowlands adjoining the channel of a river, stream or watercourse, or adjoining the shore of an ocean, lake or other body of standing water, which have been or may be inundated by flood water. Floodplains are further categorized by the frequency of flooding (discussed in more detail in a subsequent chapter). A common standard is the flood with a one percent chance of being equaled or exceeded in any given year – commonly referred to as the "one percent flood" and often inappropriately labeled the "100-year" flood. Floods, of course, are not confined to the area inundated by the one percent flood. Larger floods may, and have often, occurred, but since the 1960s the one percent flood has been generally accepted as a standard for regulation of most additional development in identified flood-prone areas (FEMA 2007).

1.2.1 OFF-PLAIN FLOODING

Off-floodplain flooding typically occurs when very intense rainfall causes high levels of surface runoff. This can occur at locations outside major floodplains, or within a floodplain where the river did not overflow, but area was flooded due to intense local rainfall. In urban areas, off-floodplain flooding can be more frequent because the high percentage of paved areas significantly increases the runoff coefficient. Sewer backups and pump failures, insufficient drainage pipe capacities, and clogged street gutters are also common causes of off-floodplain flooding.

While the definition for floodplain can refer to the area adjacent to a river that floods at a one-percent exceedance probability, it is important to note that with smaller floods, off-plain flooding can occur even on a flood plain. Similarly, with very large floods, on-plain flooding can occur in areas beyond the area covered by the one-percent exceedance probability flood envelope.

The short-term and localized nature of off-plain flooding means that heavy precipitation, even over short periods of time (e.g., hourly to daily) can be a good proxy for determining this type of flood risk.

1.3 IMPACTS OF CLIMATE CHANGE

The climate has warmed more than one degree Celsius since pre-industrial times (mid-1800s) and the warming has been attributed primarily to anthropogenic use of fossil fuels (IPCC 2021). There is growing concern that besides increased heatwaves, anthropogenic climate change is affecting other phenomena and causing more extreme weather. There is a high degree of confidence that climate change is increasing precipitation. The thermodynamic explanation is straightforward. As temperatures increase, the saturation vapor pressure of water vapor increases – more water vapor can exist in the atmosphere. The Clausius-Clapeyron relationship quantifies this behavior – about seven percent more water vapor for every degree Celsius increase. The connection to precipitation is that all else equal, precipitation should increase at the same rate. Thus, as moist air rises, there is seven percent more water vapor to condense in the form of rainfall for every degree the atmosphere is warmer.

The increases in precipitation have indeed been observed. A simple analysis of U.S. annual average precipitation in Figure 1 shows about a two-inch increase since 1900 when the annual average was 29 inches; thus, about seven percent increase. Over the same time-period, average U.S. temperatures have increased about one degree Celsius. The observed increase in precipitation almost exactly matches the expected theoretical increase from the Clausius-Clapeyron relationship.

Figure 1

TIME SERIES OF U.S. ANNUAL AVERAGE PRECIPITATION TOTALS CORRESPONDING TEMPERATURE CHANGES (HEAVY LINES AS SHOWN) AND BEST FITS FROM LINEAR REGRESSION (DOTTED LINES AND EQUATIONS).

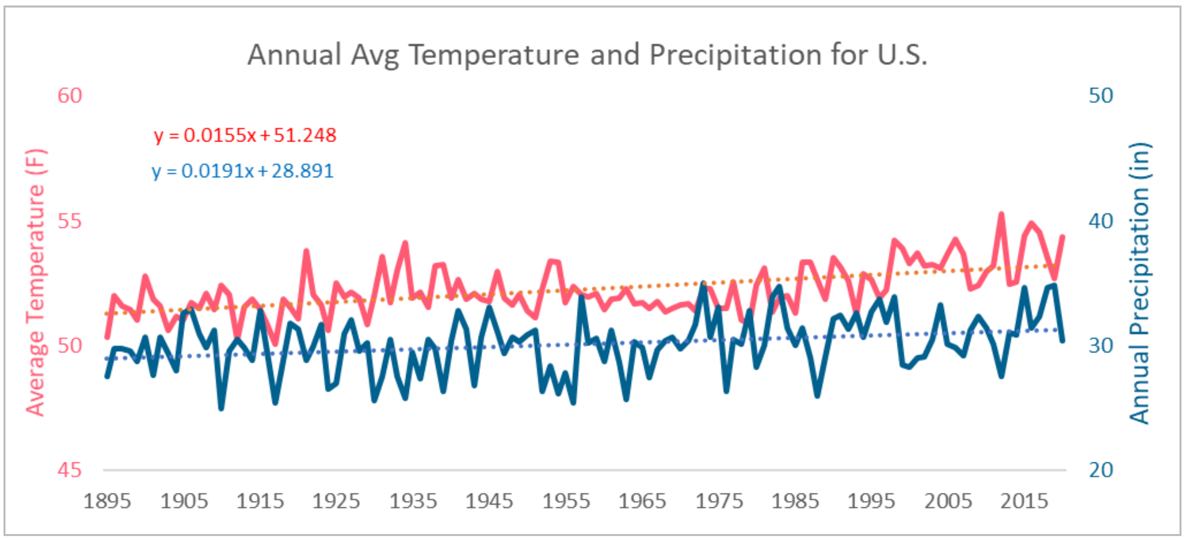

Data Source: National Oceanic and Atmospheric Administration (NOAA)

Numerous studies (e.g., Kunkel *et al.* 2010, Kunkel *et al.* 2012, Westra *et al.* 2013, Anderson *et al.* 2015, Easterling *et al.* 2016, Janssen *et al.* 2016) have confirmed increases in precipitation of one sort or another. An important aspect of understanding how climate change may impact floods is to consider how heavy precipitation events have changed, are changing, and may change in the future. These are the events that can overwhelm existing flood mitigation measures – including the capacities of rivers.

Various metrics of extreme precipitation exist based either on amounts corresponding to the 0.01 exceedance probability for a location or on standard amounts. The result does not change much qualitatively. Figure 2 below

Figure 2
COMPARISON OF HEAVY PRECIPITATION (>1 INCH/DAY) DAYS ACROSS THE U.S. FOR TWO HISTORICAL PERIODS

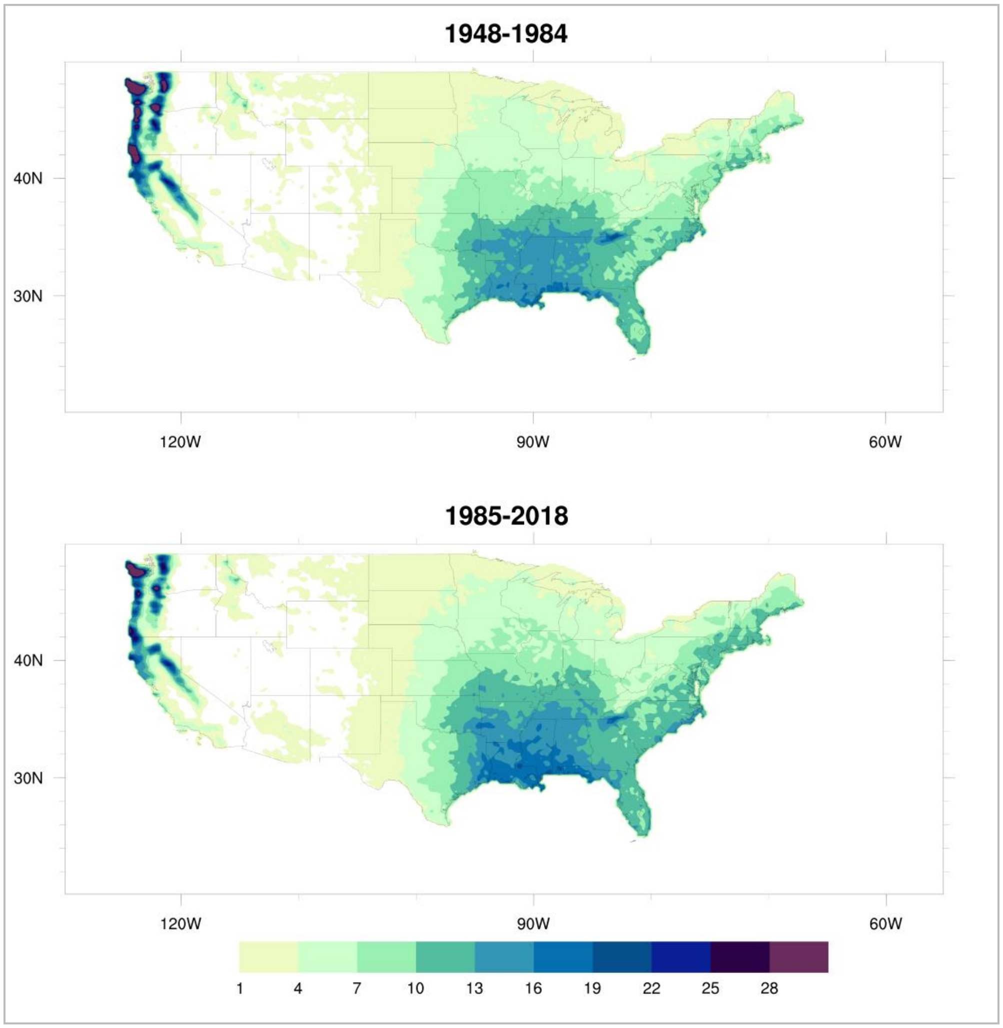

shows how the number of one-inch precipitation days has increased from the 1948-1984 time period to the 1985-2018 time period. The pattern has not changed much although wet areas have become wetter. Again, numerous studies have found similar results (e.g., Kunkel *et al.* 2010, Pall 2017). The increases in precipitation are expected to continue under various RCP scenarios, particularly the intensity and frequency of heavy events (e.g., Janssen *et al.* 2016, Prein *et al.* 2017, Myhre *et al.* 2019).

Evaluating projections for flood however, in contrast to the precipitation that is part of the process, is more complex. Off plain flooding, particularly in urban areas is less so. Heavy precipitation in an area equates to the strong likelihood of localized flooding. At the same time, especially for urban locations, the continued growth of cities, the conversion of land types with water absorbing properties to ones with less absorbent properties has to be taken into account to more comprehensively understand potential impacts of climate change on urban (and sub-urban) flooding in the future. Studies have considered the effects of both regarding projections of urban flooding, but results are made in general terms. Even for studies of future precipitation projections superimposed onto current urban and infrastructure conditions – the results are expressed in general terms.

As will be shown in the results section, off-plain flooding contributes significantly to overall flood risk, so understanding how the risk from urban flooding in terms of the overall risk is important.

For on-plain flooding, the situation is more complex. As we noted at the beginning of this report, there is more to understanding the risk of riverine flooding than just considering how precipitation may change. Once water reaches the surface, it may travel hundreds if not thousands of miles before contributing to a flood many states away and several weeks from when it first fell to earth. Thus, it is not an easy task at all to consider how flood depths may change, how flood plains may expand even by qualitatively accounting for the different effects on precipitation, wind, sunshine, and humidity, that climate change may bring.

Numerical models of varying degrees of resolution are required – climate models to provide information on the relevant quantities at sub-one-degree horizontal resolution that provide daily output are necessary but not sufficient. Surface runoff and hydrological streamflow models are also necessary. Even these models can be time consuming to run on decadal scales so coarser resolution versions are run and then the output is downscaled.

Several studies have addressed potential impacts of climate change on riverine flooding. Arnell and Lloyd-Hughes (2014) conducted a global study looking at various Representative Concentration Pathways (RCPs) combined with Shared Socio-economic Pathways (SSPs). Results from 19 different general circulation models that are part of the Coupled Model Intercomparison Project Phase 5 (CMIP5) were shown. primarily in terms of how many additional people would be impacted – from riverine flooding, water resource stress, etc. Although breakdowns by selected regions were provided, the results were very macro-scale. That said, for RCP 8.5 by 2050, it was shown by unanimous model agreement that Southeast Asia would be the most impacted – Asia in general and that 50-380 million additional people in Southeast Asia would be affected by riverine flooding. By comparison in that study, the United States showed considerably less sensitivity with a range of 0-30% additional population being impacted by riverine flooding.

Koirala *et al*. (2014) also evaluated potential climate change impacts globally but provided a bit more regional texture (at least pictorially) and from a streamflow output perspective. They used output from 11 different GCMs as input to a Catchment-based Macro-scale Floodplain Model (CaMa-Flood; Yamazaki et *al.* 2011). The study found a decrease in mean, high, and low flows across much of the western U S. with increases in the Midwest, East, and states bordering the Pacific Ocean.

Alfieri *et al*. (2016) used climatic projections from seven downscaled general circulation models (GCMs) to estimate changes in the expected damage and population affected by river floods under specific warming levels (SWLs) of 1.5 °C, 2 °C, and 4 °C as compared to the preindustrial levels. For a 2 C warming scenario they found a three-fold increase in expected damage for the U.S.

Wobus *et al.* (2017) used hydrologic projections based on the Coupled Model Intercomparison Project Phase 5 (CMIP5) to estimate changes in the frequency of modeled 1 % annual exceedance probability (1 % AEP, or 100-year) flood events at 57 116 stream reaches across the contiguous United States and linked the flood projections to a database of assets within mapped flood hazard zones to model changes in inland flooding damages throughout the U.S. over the remainder of the 21st century. They found significant increases in the frequency. They found one-hundred-year events became less than 20-year events over southern California and the upper intermountain region (Wyoming, Montana, Idaho) with comparable increases in the central Mid-west and Northeast although many surrounding locations exhibited decreased frequency. On the country scale, they found a roughly doubling in frequency a 100-year event would become a 50-year event by mid-century under an RCP 8.5 scenario. For damages, the impact was approximately a 50% increase in annual flood damage.

The First Street Foundation performed a national flood assessment for current climate conditions as well as future conditions at 2050 under the assumption of an RCP 4.5 emissions scenario using a model developed in conjunction with several groups within private industry and academia (First Street 2020a). The First Street Flood Model allows for the understanding of risk from any type of flooding event by taking into account inundation from fluvial (riverine), pluvial (rainfall), storm surge, and tidal sources at the parcel level (3m resolution). Results from the analysis for future conditions show increased flood risk almost everywhere from a few tenths of a percent to a few tens of percent. Results are provided in the context of increased number of properties at risk. The national average of percent increase in properties at substantial risk, defined in their studies as >26% chance of experiencing a (100 year) flood in a thirty-year period, was found to be ~11% (First Street 2020b) although the impacts from coastal vs. tidal vs. fluvial vs. pluvial are hard to distinguish except by inference from proximity of counties to the coast and rivers and streams.

Section 2: Leveraging the AIR Inland Flood and Hurricane Models

Two AIR models form an integral part of this study: the AIR Inland Flood Model for the United States and the AIR Hurricane Model for the United States. The AIR Inland Flood Model represents the view of inland flood risk for the current climate (2020) for all sources of precipitation except hurricanes. The AIR Hurricane Model for the U.S. represents the view of hurricane risk for the current climate (2020) and accounts for property damage from wind, storm surge and inland flooding from hurricanes. Below we describe how flooding is modeled in the AIR Inland Flood Model. The modeling of flood is similar in the AIR Hurricane Model.

The Inland Flood Model simulates the property damage caused by precipitation-induced flooding on insurable and insured properties in the contiguous U.S. from various types of weather systems including extratropical cyclones, weather fronts, isolated thunderstorms, etc. (hurricane precipitation is accounted for separately). It is a fully probabilistic, event-based inland flood model that accounts for on- and off-plain flooding. It captures both large-scale and highly localized floods, including flash floods that result from short-lived but extreme precipitation. The model is built to meet the wide spectrum of flood risk management needs in the insurance industry and accounts for policy conditions specific to the United States. The model captures all the complexities inherent in a flood generation process to determine the amount of water that accumulates over land as excess runoff and drains into rivers. The contributing factors include the space-time patterns of rainfall, the effects of a highly variable climate, snowmelt, topography, local geology, soil type, antecedent conditions, land use and land cover, and other local factors. The modeling process accounts for the effects of man-made flood defenses and flood regulation, and/or reservoir diversions.

Precipitation for the flood model is computed using a coupled General Circulation Model (GCM) and a Numerical Weather Prediction (NWP) model. The AIR model identifies separate flood events through the use of a clustering algorithm that divides flood occurrences spatially and temporally, representing the physical realities of flood. To accommodate widely used methods of event identification for insurance purposes, the model incorporates the 168 hours clause by dividing on-floodplain events. As a result, the majority of these events are less than 168 hours in duration. Through the use of this algorithm, nearly one-half million separate flood events are included in the model's 10,000-year catalog.

For local intensity, damage, and loss estimation, the model features a physically based hydraulic model that incorporates the 18 hydrological regions covering the contiguous United States as well as contributing areas in Canada and Mexico. This hydrological domain covers a total area of approximately 8.2 million km2 (3.2 million mi^2) and includes detailed river networks extending over 2.2 million km (1.4 million mi), with approximately 335,000 distinct unit catchments. It includes every stream with a drainage area of at least 10 km2 (3.9 mi^2). To accurately assess flood risk along streams and creeks with drainage areas smaller than a 10- km^2, the model uses physically based pluvial flood modeling at a 10-m resolution throughout the model domain.

The flood depths are used with AIR developed damage functions that determine the percent damage for given flood depths according to building characteristics such as construction type (wood, brick, etc.), occupancy (residential, commercial, etc.), elevation above ground, number of stories, and year built. An Industry Exposure Database, also developed at AIR, is used to determine damage for all properties in the U.S. at 90 m resolution. The database contains information on all property considered insurable from a structural and use standpoint including buildings for residence, commerce, and industry and includes mobile homes, automobiles, and contents within structures. Flood loss by event can be separated into on- and off-plain components.

The AIR Hurricane Model is a fully stochastic model consisting of 10,000 years' worth of simulated hurricanes, which have wind speeds of at least 74 mph. The model leverages information on more than 1,000 historical storms that have occurred in the Atlantic basin from 1900 to 2018. This information is from the North Atlantic Hurricane Databases HURDAT and HURDAT2 (NHC, 2021). The model supports two types of catalog, a Standard catalog reflecting hurricane risk under average current climate conditions, and a Warm Sea Surface Temperature (WSST) catalog reflecting hurricane risk under warmer-than-average sea-surface temperatures. As with the AIR Inland Flood Model, losses due to on- and off-plain flooding are simulated at a 10-meter resolution. On-plain flood losses are determined by the extent to which rivers exceed their capacity and are not limited by agency definitions of the extent or locations of flood plains (e.g., regions that have a 1% exceedance probability of being flooded as determined by the Federal Emergency Management Agency FEMA). More information about the AIR Hurricane Model is available online at the Florida Commission on Hurricane Loss Projection Methodology (FCHLPM, 2021).

Section 3: Methodology

Since the mechanisms that cause on-plain flooding are different from those which cause off-plain flooding, separate on-plain and off-plain views of future flood risk are developed in this study. Riverine flood maps generated from five different GCMs as part of CMIP5 are used to evaluate future changes in on-plain flood depths and extents. Daily precipitation data, downscaled from the same GCMs, are used to evaluate how heavy precipitation events could cause off-plain flooding to change. Probabilistic hazard views for the current climate are combined with probabilistic loss views from the AIR models to create county-specific on- and off-plain damage functions. The damage functions are then used in conjunction with probabilistic hazard views for 2050 under RCP 8.5 to determine future probabilistic loss views. Here we list the data used and describe how this data was processed to create a projected view of inland flood loss risk under RCP 8.5 at 2050.

3.1 DATA SOURCES

Hazard data, obtained from two external sources, are used to create probabilistic views of on-plain and off-plain flood hazard risk for the current climate (2020) and the climate at the scenario-horizon RCP8.5-2050. Loss data, obtained from two AIR models, are used to create probabilistic views of on-plain and off-plain flood loss risk for the current climate (2020). These data sources are used to create probabilistic views of the on-plain and off-plain flood loss risk at RCP8.5-2050. Below we describe in more detail the sources of hazard and loss data.

3.1.1 ON-PLAIN HAZARD DATA

The on-plain hazard data for the current climate and future projections is provided by Aqueduct Floods (Ward *et al*., 2020). This is an online platform that measures riverine and coastal flood risks at a historical baseline of 1980 and future projections of 2030, 2050, and 2080 for RCPs 4.5 and 8.5. The platform was developed by a public-private consortium and is funded by the Netherlands Ministry of Infrastructure and Water Management and the World Bank.

For this study we downloaded Aqueduct Version 2 riverine flood maps at nine return periods for three time-horizons and one RCP for five GCMs, as well as the same flood maps for the baseline of 1980. The specific return periods, horizons and GCMs are listed in Table 1. The data were downloaded from http://wri-projects.s3.amazonaws.com/AqueductFloodTool/download/v2/index.html on 13th April 2021. The five GCMs are written in short name format in Table 1. Their long names are provided in Table 2.

Table 1

SUMMARY OF THE ON-PLAIN HAZARD DATA SOURCED FROM AQUEDUCT FLOODS.

Flood type	Scenarios	Horizons	Return periods	GCMs (short name)
Riverine	Historical, RCP 8.5	1980, 2030, 2050	2, 5, 10, 25, 50, 100, 250, 500, 1000	NorESM1-M, GFDL-ESM2M, HadGEM2-ES, IPSL-CM5A-LR, MIROC-ESM-CHEM

Table 2

SHORT AND LONG NAMES OF THE GLOBAL CLIMATE MODELS (GCMS) USED IN THIS REPORT.

GCMs (short name)	GCMs (long name)
NorESM1-M	Norwegian Climate Centre Earth System Model M
GFDL-ESM2M	NOAA Geophysical Fluid Dynamics Laboratory Earth System Model Version 2M
HadGEM2-ES	Hadley Centre Global Environment Model version 2
IPSL-CM5A-LR	Institut Pierre Simon Laplace Model CM5A-LR
MIROC-ESM-CHEM	University of Tokyo, National Institute for Environmental Studies, and Japan Agency for Marine-Earth Science and Technology Earth System Model Chemistry

The following description of the Aqueduct Floods hazard modeling methodology is taken from Ward *et al*. (2020).

The on-plain hazard maps were created by Aqueduct Floods using the Global Flood Risk with IMAGE Scenarios (GLOFRIS, Ward *et al.* 2013, Winsemius *et al.* 2013) modeling framework. These are inundation maps showing the flood depth and extent at a resolution of 30 x 30 arc seconds which is about 1 km at the equator. GLOFRIS applies a global hydrological model called PCRaster Global Water Balance (PCR-GLOBWB, Sutanudjaja *et al.* 2018) with a river and floodplain routing scheme to make long-term simulations of discharges and flood levels for different climate conditions. The hydrological model accounts for precipitation, evaporation (e.g., from soil, plants, etc.), and runoff (e.g., from snowmelt, surface, etc.)

The meteorological data used to create the historical baseline (1980) simulations are the 1960-1999 reanalysis data taken from the European Union Water and Global Change (EUWATCH) program. The meteorological data for the five GCMs are taken from the Inter-sectoral Impact Model Intercomparison Project (ISIMIP). The EUWATCH and ISIMIP data is used to force PCR-GLOBWB over various time periods between 1950 and 2099. The view at each horizon is based on the forty years around the horizons. For example, the 2030 is based on the years 2010-2049 and 2050 is based on 2030-2069. It is important to recognize that our analyses are based on average conditions over a 40-year period centered around 2050 rather than conditions that may exist right at 2050.

Extreme value statistics are then applied to the PCR-GLOBWB output to derive the on-plain water volumes per grid cell for the nine return periods. The extreme value distribution from each GCM is bias corrected using the distribution created from the EUWATCH data. The corrected future view, for example, is the historical view from EUWATCH plus the difference between the historical and future GCM views.

The flood volumes at each return period are used as input to a volume spreading flood model to convert the flood volumes at a 5 x 5 arc minute (about 10 km) resolution to the 30 x 30 arc second resolution.

The Aqueduct maps provide global coverage but for this report we only use the data in the contiguous United States.

3.1.2 OFF-PLAIN HAZARD DATA

The on-plain flood maps provided by Aqueduct Floods are annual occurrence maps, so we seek to create the same view for the off-plain flood hazard risk. Given that in AIR's Inland Flood Model for the U.S., an event's off-plain flood footprint is simulated from the maximum 24-hour cumulative precipitation during that event, we decide to use the annual maximum daily precipitation to determine future off-plain annual occurrence losses.

We decided to use the MACAv2-METDATA provided by the University of Idaho which is the same source that provides the Vapor Pressure Deficit data in the companion study on U. UUSS. Wildfire risk (Sousounis *et al.*, 2021). The dataset draws climate forcings from a statistical downscaling of GCM data from the Coupled Model Intercomparison Project 5 (CMIP5) (Taylor *et al.* 2012). The Multivariate Adaptive Constructed Analogs (MACA) method is a statistical downscaling method which uses an observational dataset called METDATA for bias-correction and matching spatial patterns in climate model output (Abatzoglou and Brown, 2012). MACAv2-METDATA contains downscaled, bias-corrected historical (1950-2005) and projected RCP 8.5 (2006-2099) data for up to 20 GCMs. The observational METDATA spans the period 1979–2019 and blends spatial attributes of climate data from PRISM7 with desirable temporal attributes from regional reanalysis (NLDAS-2) (Abatzoglou, 2011).

For the present report we downloaded data for the same five GCMs listed in Table 2. The datasets are high-resolution (4-km) gridded datasets of daily cumulative precipitation that span the conterminous US. The MACAv2-METDATA datasets for the five GCMs were downloaded from http://thredds.northwestknowledge.net:8080/thredds/fileServer/MACAV2/ over 6th to 10th May 2021, while the METDATA dataset was downloaded from https://www.northwestknowledge.net/metdata/data/ on 4th May 2021.

The procedure used to create annual occurrence maps of the maximum daily precipitation is described in 3.2.1.2 Off-plain hazard.

3.1.3 ON-PLAIN AND OFF-PLAIN LOSS DATA

Insurable losses due to buildings and contents damage and business interruption are computed by running AIR's U.S. industry exposure database through Touchstone 2020, the 2020 vintage of AIR's detailed modeling platform.

The industry exposure is AIR's proprietary database of all insurable properties in the United States. It includes properties from four lines of business namely residential, commercial, automobiles and mobile homes. The residential line includes one-to-four family homes and apartment contents. The commercial line includes buildings and contents from a wide range of sectors including, but not limited to, mining, manufacturing, utilities, retail, and professional services. It also includes apartment buildings and large industrial facilities. AIR's U.S. industry exposure for flood modeling has a resolution of 90 meters.

We used AIR's Inland Flood Model for the U.S. to obtain non-hurricane inland flood losses and AIR's Hurricane Model for the U.S. to obtain hurricane inland flood losses. For both models we used 10,000-year stochastic catalogs and for U.S. hurricane we selected the Standard catalog which reflects hurricane risk under average current climate conditions.

The procedure for creating the RCP8.5-2050 view of risk, as discussed later in this section, is performed at a county resolution, so we output 10,000 years-worth of event losses from Touchstone at a county level, split into on-plain and off-plain, and non-hurricane and hurricane. Note that losses from Touchstone can be output at a range of resolutions from individual properties to country and multiple country levels.

County resolution was chosen as a compromise between retaining the high-resolution information in the Aqueduct and MACAv2 data (1-4 km) and reporting losses at a low enough resolution that enables actuaries to apply the results to their business. Upscaling hazard data from a high to a very low resolution could dilute important and meaningful signals in the hazard data but counties in the U.S. are generally small enough to retain this information.

The loss datasets from Touchstone 2020 represent a probabilistic view of the risk for the current climate in 2020.

3.2 PROCEDURES

Here we describe the steps taken to create a probabilistic view of the inland flood risk for RCP8.5-2050 using the hazard and loss data described in section 3.1Data sources.

3.2.1 OCCURRENCE EXCEEDANCE PROBABILITY COUNTY MAPS

In the first step, on- and off-plain hazard data from the sources described above, and loss data from the AIR Model are combined to create annual Occurrence Exceedance Probability (OEP) curves for every county in the conterminous US. Below we describe the sub-steps taken for the on-plain hazard, the off-plain hazard, and both the on- and off-plain losses.

3.2.1.1 On-plain hazard

From the Aqueduct Data, there is one set of on-plain hazard OEP maps for 1980 where each map is a different return period. There are five sets of equivalent maps for RCP8.5-2030 and five sets for RCP8.5-2050 where each set is a different GCM. We require a set of maps that represent the county-level on-plain hazard OEP for the present-day 2020 and a set of equivalent maps for RCP8.5-2050.

First, we aggregated the 1 km resolution maps to county-level for 1980, 2030 and 2050, then we linearly scale the 1980 maps by the 2030 maps to obtain the 2020 maps.

The 1 km maps are aggregated to county-level by aggregating the flood depths of all the cells that lie within each county at each return period. The counties are at a high enough resolution to distinguish the major rivers in the U.S. Correlation across the grid points within a given county is assumed when combining the flood depths at 1 km resolution.

Five sets of maps for 2020 are calculated using the following formula for each return period at each county:

$$h_{2020} = h_{2030} - \frac{2030 - 2020}{2030 - 1980}(h_{2030} - h_{1980}), \tag{1}$$

where h_{2020} is the aggregated flood depth at a given county for a given GCM for 2020, h_{2030} is the equivalent for 2030, and h_{1980} the same for 1980.

Three additional maps, representing return periods 2,500; 5,000; and 10,000 years, are created for each set by extending the OEP curves at each county. This is achieved by modeling the OEP distribution as a Gumbel distribution:

$$x = 1 - \exp\left[-\exp\left(-\frac{h - a}{m}\right)\right], \tag{2}$$

where x is the probability that the county flood depth exceeds h, and m and a are unknown parameters whose values are obtained by fitting the model to the OEP curves. Aqueduct Floods includes flood defenses which manifests in OEP curves that jump from zero depth to a large finite depth at return periods of 100 and 250 years and above. These OEP curves are modeled using the Gumbel distribution and exceedance probabilities with finite flood depths. For example, if the flood defenses in a county prevent flooding up to the 100-year return period, the Gumbel distribution is fitted to this county's depths at 250, 500 and 1,000 years.

This results in five sets of twelve return period maps for 2020 and RCP8.5-2050 containing the county aggregated flood depths. The change in OEP curves between these two scenario-periods can be used to guide the change in

OEP curves for loss, however since the hazard curves are from Aqueduct Floods and the loss curve for 2020 from AIR, there can be mismatches between the two datasets. For example, according to Aqueduct Floods some counties have zero flood depths across their entire OEP curves but those same counties produce loss OEP curves from AIR's models. One reason for this is that AIR's models simulate hazard and therefore loss at 10 meters, a much higher resolution that the 1 km resolution of Aqueduct Floods. For these counties it is decided to augment the Aqueduct Floods data by assigning the OEP curve of their nearest neighboring county that has a non-zero flood depth OEP curve. The change in OEP curve of these counties will be the same as those of their nearest neighbor.

For some other counties, the OEP curve jumps from zero to a finite flood depth at the standard of protection (SOP) of the flood defenses. To avoid zeroes in the data, we assign a nominally low flood depth to the flood depths below the SOP.

Following this data augmentation, the mean of the five OEP curves at each county is computed for both 2020 and RCP8.5-2050. This provides a single on-plain hazard OEP curve for each county in each scenario-period. The next section describes the procedure for creating the same views for the off-plain hazard.

3.2.1.2 Off-plain hazard

As with on-plain, we require a set of maps that represent the county-level off-plain hazard OEP for 2020 and RCP8.5-2050. The maps for 2020 are derived from the years 2000 to 2039. The data from 2000 to 2005 are sourced from each GCM's historical simulation while the data from 2006 to 2039 are sourced from each GCM's RCP 8.5 simulation. The maps for RCP-2050 are derived from the years 2030 to 2069.

First, the daily precipitation accumulated in each county is calculated by summing the daily precipitation data over all cells that lie in each county. For each county we find the maximum daily precipitation in every year from 2000 to 2069. Generalized extreme value (GEV) distribution functions are fitted to each forty-year period using L-moments estimation. L-moments estimation is preferred to Maximum Likelihood Estimation (MLE) because it gave more sensible values at the higher return periods than MLE which was more sensitive to the observations in some counties. However, both methods give similar fitted curves for most counties. The accumulated precipitation values are read from the fitted curves for the same twelve return periods used for the on-plain analysis. The calculations are repeated for all five GCMs over the years 2000 to 2039 and 2030 to 2069.

3.2.1.3 On-plain and off-plain loss

The county-level event losses sourced from Touchstone are used to create count-level loss OEP curves for 2020. For each county, we find the maximum event loss in each year of the 10,000-year catalogs and rank those years to assign find the losses at the twelve return periods used in this study. This results in one set of county-level on-plain loss OEP curves and one set of county-level off-plain loss OEP curves.

3.2.2 COUNTY-LEVEL DAMAGE FUNCTIONS

In the second step, we create on-plain and off-plain damage functions that are specific to each county. These functions relate hazard to loss and enable us to estimate future loss projections based on future hazard projections. The procedure, which can be used for either on-plain or off-plain data, is illustrated by the schematic in Figure 3.

Figure 3
SCHEMATIC ILLUSTRATING HOW TO QUANTILE MAP HAZARD (A) AND LOSS (B) OEP CURVES TO CREATE A DAMAGE FUNCTION (C).

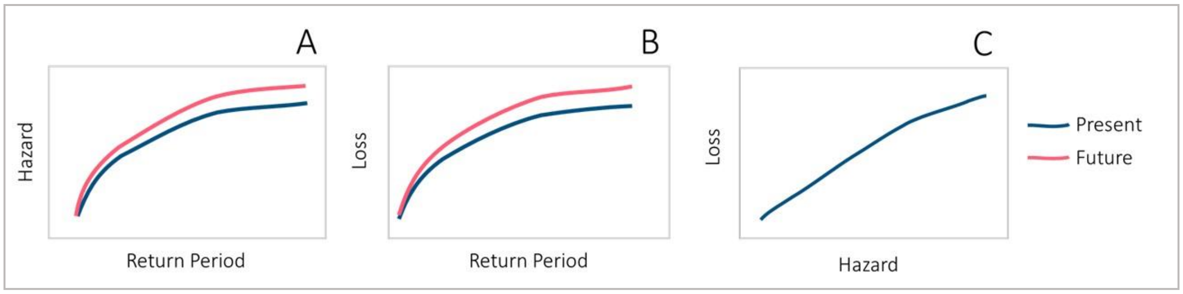

The quantiles of the hazard OEP curves for 2020 (blue line in Figure 3A) are mapped to the loss OEP curves for 2020 (blue line in Figure 3B) to create damage functions (blue line in Figure 3C) for each county. These functions relate hazard to loss and since we are assuming that the exposure does not change between 2020 and 2050, the functions are *time-invariant*. Therefore, the damage functions provide a means of relating the hazard OEP curves for RCP8.5-2050 (pink line in Figure 3A) to the loss OEP curves for that same scenario-period (pink line in Figure 3B).

Note that this method can also account for changes in the total replacement value of the exposure over time. The county-level loss OEP curves for 2020 would need to be converted to damage ratio OEP curves where damage ratio is defined as the ratio of the county loss to the total replacement value in that county. Since this report is solely concerned with quantifying the change in loss due to climate change alone, the exposure in RCP8.5-2050 is assumed to be the same as in 2020 so it is unnecessary to convert loss to damage ratio. Below we demonstrate the procedure using the on-plain and off-plain OEP curves.

3.2.2.1 On-plain

For most counties the hazard and loss OEP curves are *absolutely monotonic* meaning that their values always increase with return period. This is an ideal case for quantile-mapping. Figure 4 below shows an example of this for St. Charles county, Missouri.

Figure 4
ON-PLAIN HAZARD (A) AND LOSS (B) OEP CURVES FOR ST. CHARLES, MISSOURI FOR 2020 AND RCP8.5-2050 USED TO CREATE THE ORIGINAL AND EXTRAPOLATED DAMAGE FUNCTIONS (C).

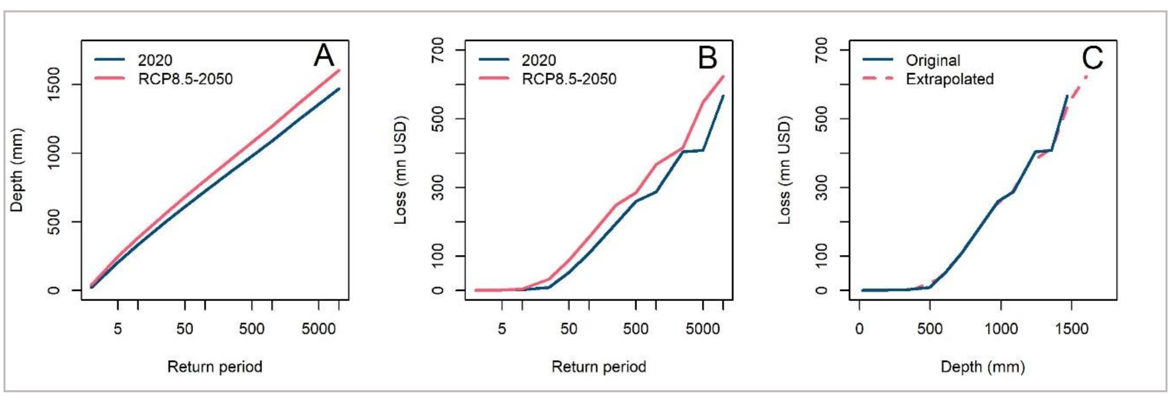

For some counties, the hazard or loss OEP curves are weakly monotonic which means their values may increase or not change with return period. Hazard or loss values can be zero up to a critical return period either because the county is not regularly flooded, or flood defenses have been installed to prevent flooding up to the SOP. Since the hazard and loss data are from two different sources, there can be disagreement as to whether a county experiences flooding and at what return periods.

Figure 5 shows an example taken from Jefferson Davis, Mississippi, a county that is not regularly flooded. The Aqueduct model finds that for the 2 and 5-year return periods there is no on-plain flooding in the county, but the AIR model finds that on-plain flooding does occur at the 5-year. The damage function suggests that loss can vary up to 90k USD in this county even if no significant flooding occurs. In this county, the future hazard OEP shows no on-plain flooding up to the 50-year return period. The future 2 and 5-year return periods are mapped to the 2 and 5-year losses from 2020 and the future 10 to 50-year losses are mapped to the 5-year loss from 2020.

Figure 5

ON-PLAIN HAZARD (A) AND LOSS (B) OEP CURVES FOR JEFFERSON DAVIS, MISSISSIPPI FOR 2020 AND RCP8.5-2050 USED TO CREATE THE ORIGINAL AND EXTRAPOLATED DAMAGE FUNCTIONS (C).

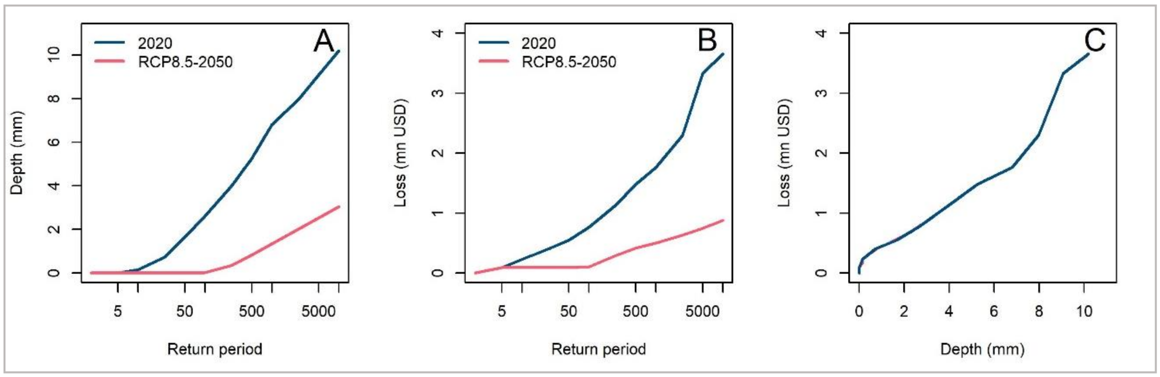

It should also be noted that while the loss values are an accurate representation of county losses caused by simulated on-plain flooding events, the hazard values are approximations of county flood depths. The flood depths in Aqueduct's 1 km on-plain OEP maps are not caused by a single on-plain flood event but would be caused by multiple events occurring at different times. The aggregated county flood depths used in this report are therefore an overestimate of the true county on-plain flood depths at those return periods. However, this approximation is acceptable for our case because we are using the relative change in on-plain flood OEP curves to infer the relative change in the losses.

3.2.2.2 Off-plain

The off-plain hazard values used in this report are an accurate representation of off-plain flood depths. In almost all counties, the off-plain hazard and loss OEP curves are absolutely monotonic. Figure 6 shows an example of off-plain OEP curves and damage function, taken from Butte county, California. The damage functions created from present-day hazard and loss OEP curves (blue line in Figure 6C) are initially restricted to the range of hazard and loss values in the present-day data. This damage function could only infer losses up to present-day 10,000-year flood depth. To overcome this limitation, we extrapolate the damage functions in those counties where the 10,000-year hazard in RCP8.5-2050 is greater than that in 2020.

Figure 6

OFF-PLAIN HAZARD (A) AND LOSS (B) OEP CURVES FOR BUTTE, CALIFORNIA FOR 2020 AND RCP8.5-2050 USED TO CREATE THE ORIGINAL AND EXTRAPOLATED DAMAGE FUNCTIONS (C).

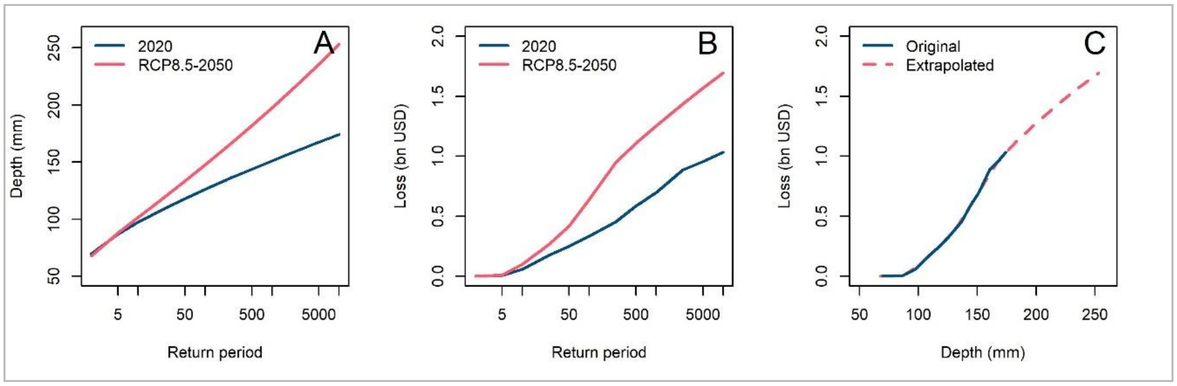

The extrapolation is performed by fitting the following formula to the quantiles at the 2,500, 5,000 and 10,000-year return periods in the hazard OEP curves:

$$y = n \ln h + b, \quad (3)$$

where *y* is the loss, *h* is the hazard value, and *n* and *b* are fitted parameters. This extrapolation is applied to both on-plain and off-plain damage functions, but it is more frequently used for off-plain where the hazard increases in more counties than the on-plain. None of the extrapolated losses exceed the total replacement value in the county. An extrapolated damage function is shown in Figure 6C (pink, dashed line). The loss OEP curve for RCP8.5-2050 (pink line in Figure 6B) demonstrates that the extrapolated damage function gives sensible results.

3.2.3 LOSS PERSPECTIVES

At this point we have created on-plain and off-plain county-level occurrence losses for twelve return periods. Additional loss perspectives can be computed from this rich dataset. Below we describe the procedures for creating these extra perspectives.

3.2.3.1 Average annual occurrence loss

The average annual occurrence loss (AOL) is equal to the integral of the product of the annual occurrence loss and the probability of that loss occurring in a given year. We estimate this by numerical integration. The AOL of a given county for a given plain type (on or off) is calculated from:

$$\text{AOL} = \sum_{i=1}^{i=12} y_i p_i \, , \quad (4)$$

where y_i is average exceeded loss over two return periods, p_i is the difference in cumulative probability over the same two return periods, and *i* is the midpoint between each pair of the twelve return periods plus a return period of one where the exceeded loss is zero. This approximation is needed to estimate the AOLs for RCP8.5-2050. The actual modeled AOLs for 2020 can be computed from AIR's models. Figure 7 shows a comparison of how AOLs estimated from twelve return periods compares with those calculated accurately from an event loss table. The approximate method gives a reliable estimate of the actual AOLs with slight overestimation. This provides confidence that the approximation outlined above is an accurate method for calculating the county AOLs for RCP8.5-2050.

Figure 7
COMPARISON OF ACTUAL AND ESTIMATED MODELED AVERAGE OCCURRENCE LOSSES FOR ON-PLAIN (A) AND OFF-PLAIN (B) FOR 2020 FOR COUNTIES IN CALIFORNIA.

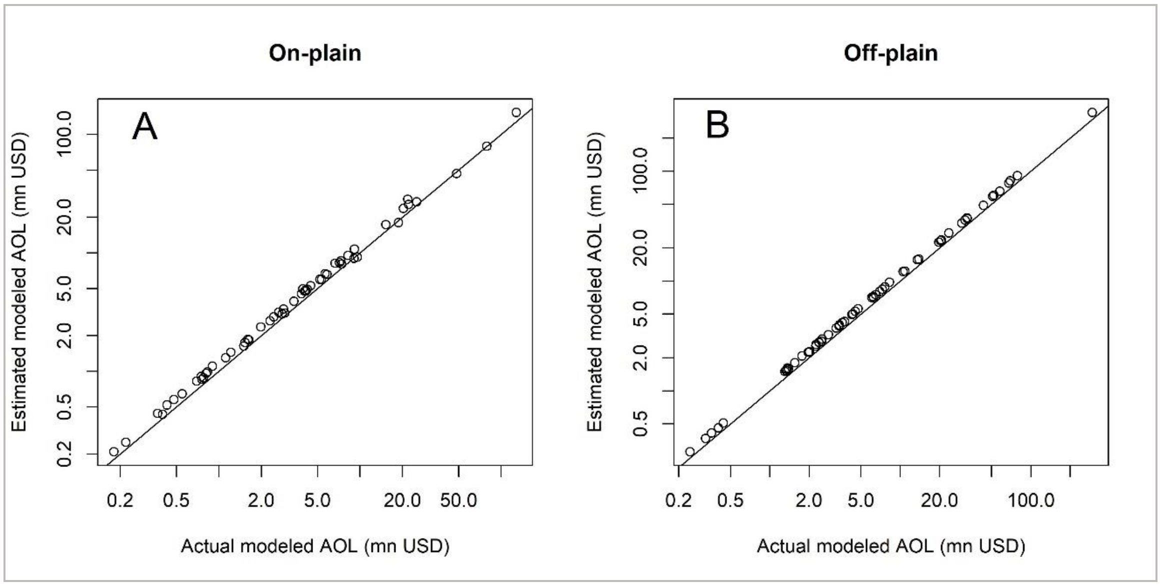

3.2.3.2 State and national losses

Here we describe a method of *upscaling* county AOLs to estimate AOLs at state and national levels, where upscaling means to estimate losses at a lower geographical resolution from losses at a higher geographical resolution.

If none of the counties in a state experience a loss at the same time, their county losses are perfectly uncorrelated, and it follows that the occurrence loss in the state is the maximum occurrence loss of the counties in that state. An example of this might be a large state with many counties that experience small floods confined to each county. However, if all the counties in a state experience a loss simultaneously, they are perfectly correlated, and the maximum occurrence loss in the state is the sum of the occurrence losses of all the counties in that state. For example, a small state with few counties that experience large floods that span all the counties. The actual state-level occurrence loss is between these two bounds, and can be approximated as a linear combination of the two:

$$y_s = wy_c + (1-w)y_u \,, \tag{5}$$

where y_s is the state AOL, y_c is the sum of the AOLs of the counties in that state, y_u is the maximum AOL of the counties in that state, and w is a weighting fraction. Each state will have two weighting fractions, one for the on-plain loss and another for the off-plain loss. The weighting fractions of each state can be calculated using the event loss tables obtained from AIR's models. If we assume the weighting fractions are the same in 2020 as in RCP8.5-2050, we can use them to calculate on- and off-plain, state-level AOLs for RCP8.5-2050 from the on- and off-plain, county-level AOLs for that scenario-horizon.

In a similar way state-level AOLs can be upscaled to estimate a national AOL. This can be repeated for each flood plain type, to give on- and off-plain, national AOLs for 2020 and RCP8.5-2050.

It is found that across the 49 states in the conterminous U.S., the county losses within each state are strongly correlated with a weighting fraction of at least 0.64 for on-plain and 0.77 for off-plain. State losses are less correlated at the national-level with a weighting fraction of 0.47 for on-plain and 0.51 for off-plain.

Section 4: Results

We provide occurrence loss change results by county, state, and at the national level at select return periods with supporting information from how the hazard changes in this study. Percent changes in loss for both on- and off-plain by county are computed as the ratio of the difference in loss between 2050 and 2020 for that county divided by the 2020 loss for that county from the AIR Model. County-level changes of occurrence loss were then aggregated to state and national levels using information about correlations between county, state, and the U.S. from the AIR Model. To aid the reader, a map of the states and major rivers in the contiguous U.S. is provided in Appendix A.

4.1 COUNTY LEVEL

The nature of the methodology in this study implies that the impact of climate change – via the change in heavy precipitation for off-plain, and the changes in flood area and depth for on-plain, align quantitatively with changes to loss, although the magnitude of the loss for a given change in hazard even from a relative standpoint will depend on the nature of the damage functions and whether flood defenses have been exceeded. We therefore first present changes in the hazard metrics for both off- and on-plain flooding at the county level at which they were derived. Figure 8 shows the on-plain view of the hazard risk for 25, 50, and 100-year return periods for 2020 and the changes for these return periods from 2020 to 2050. Figure 9 shows the same for the off-plain hazard.

The on-plain view shows the current hazard risk for on-plain flooding from the mean GCM view from the Aqueduct Floods data. A quick glance at the results for 2020 county-average flood depths for the different return periods shows similar but enhanced patterns (greater depths) with increasing return period. The highest depths are located along the Missouri and Mississippi Rivers through the heart of the U.S., with other notable depths located along major rivers running through OK, MO, and LA that feed into the Mississippi River. Other river networks, on the east side of the Mississippi, that feed into it, also show areas that are prone to on-plain flooding.

Future increases in on-plain RP flood depth are highest along the Missouri and Mississippi Rivers. Decreases are shown for the other river networks on the west side of the Mississippi River that are currently flood prone, and little change is found in RP flood depths in the on-plain flood prone regions for the rivers on the east side that feed into the Mississippi – for the most part.

The off-plain view shows county-average return period precipitation values (depths). Wettest areas include the Pacific Northwest region, the Mid-Atlantic region, and the Gulf Coast states. Precipitation values increase with increasing return period although the patterns do not change. Results for other return periods, although not shown, exhibit the same pattern. Changes in precipitation (e.g., changes in hazard) exhibit similar patterns for the return periods also, although with more regional structure. For example, all of the west coast states (WA, OR, CA) and even NV indicate increases in return period precipitation, from Canada down to Mexico. This result is suggestive of wetter mid-latitude storms, especially during the cool season, that may be attributed to increased available moisture from the Clausius Clapeyron effect, stronger storms, or slower ones. The intermountain region (ID, MT, WY, UT, CO, AZ, and NM) shows evidence of reduced RP precipitation values. Farther east, including the Great Plains, the Midwest, and Gulf states, show increases in RP precipitation values over more area than decreases. Most notable increases occur along the Gulf Coast states including east Texas and a narrower swath farther north across the same longitude range. The former may be the result of wetter tropical cyclones while the latter could be a result of increased mid-latitude storm track activity in winter. The location of the decrease/increase region through the lower Midwest suggests a northward shift of the storm track, which is consistent with a poleward migration of the jet stream. Along the East Coast, excluding Florida, there are alternating regions that show increases along the Southeast U.S. coast, decreases across MD, DE, NJ, and eastern PA, and then increases for the most part in the New England States (CT, RI, MA, VT, NH, and ME).

Figure 8

MEAN GCM COUNTY-AVERAGED 2020 FLOOD DEPTH (LEFT COLUMN) AND 2050-2020 FLOOD DEPTH DIFFERENCES FOR ON-PLAIN FLOODING FOR RETURN PERIODS AS SHOWN.

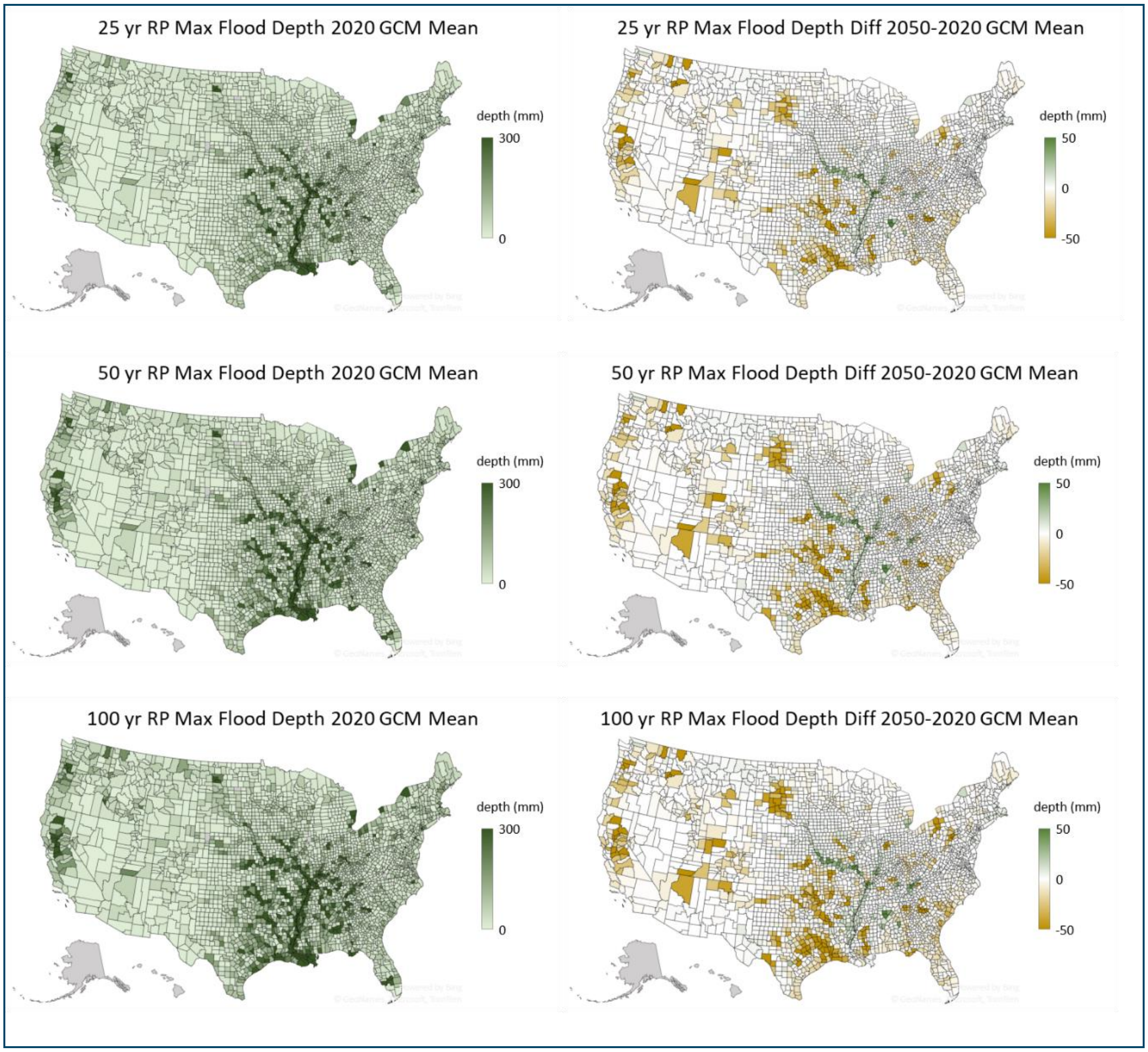

County level Average Occurrence and 100-year RP on- and off-plain flood losses from the AIR Model are shown in Figure 10. Actual numbers cannot be disclosed but the color scale is logarithmic and ranges from USD 1 million to 10 billion. In comparing the 100-year RP losses with the corresponding RP hazard plots in Figure 8 and Figure 9, it can be seen that there is not a lot of correlation, which stems primarily from the distribution of exposure. Areas with low flood risk can generate high loss in areas of high exposure.

Figure 9

MEAN GCM COUNTY-AVERAGED 2020 PRECIPITATION DEPTH (LEFT COLUMN) AND 2050-2020 PRECIPITATION DEPTH DIFFERENCES FOR OFF-PLAIN FLOODING FOR RETURN PERIODS AS SHOWN.

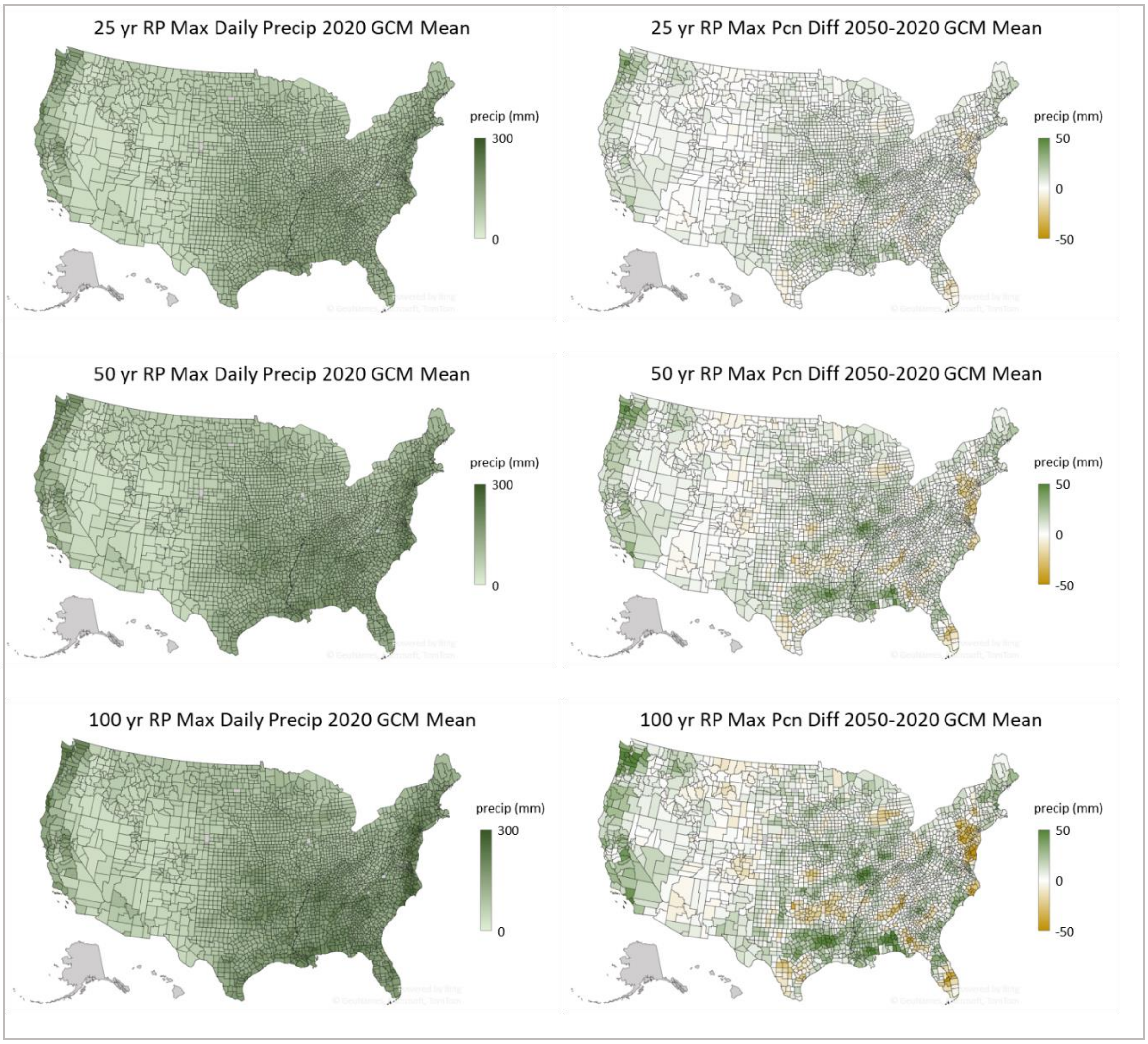

Thus, highest county losses tend to occur in urban areas such as Los Angeles, Phoenix, Denver, Houston Minneapolis, Chicago, much of the Florida peninsula, and the Northeast corridor from Washington, D.C. northward to Boston as a few examples. Differences do exist between on- and off-plain losses in these as well as other regions. For example, St. Louis, MO shows higher losses from on-plain rather than off-plain flooding because of its proximity to the confluence of the Missouri and Mississippi Rivers. Florida shows more loss from off-plain flooding rather than on-plain flooding because of its absence of rivers and because most heavy precipitation comes from landfalling and bypassing tropical cyclones. A similar explanation holds for the Northeast although heavy precipitation can also come from extratropical cyclone activity as well.

Figure 10

2020 COUNTY-LEVEL AVERAGE OCCURRENCE LOSS (LEFT COLUMN) AND 100 YEAR RP OCCURRENCE LOSS (RIGHT COLUMN) FOR ON-PLAIN FLOODING (TOP ROW) AND OFF-PLAIN FLOODING (BOTTOM ROW). LEGEND IS LOG SCALE AS SHOWN.

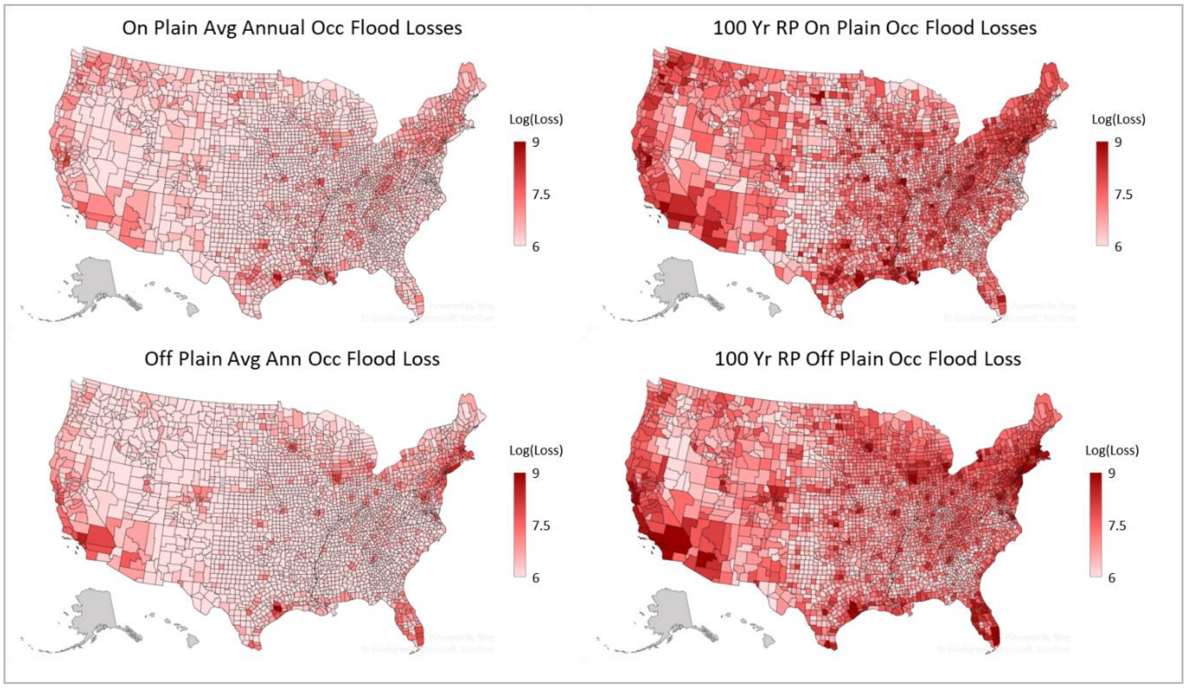

The return period on-plain occurrence loss changes are shown in Figure 11 for the mean GCM view. Several return period losses are shown to illustrate the fact that the pattern of change is relatively insensitive to return period. County level average occurrence losses will be shown later in this section owing to the way they had to be calculated. Comparison of the 100-year RP loss result with the mean GCM change in on-plain hazard shown in Figure 8 shows strong agreement. For the most part, areas with higher 100-year RP county average flood depth show increases in 100-year RP occurrence losses: namely the lower Missouri and lower Mississippi River basins, the Wabash and the River (western Indiana). Other multi-county areas that also show increases in 100-year RP on-plain flood loss include Nevada (numerous small rivers), southern Arizona (Lima River Southwest of Phoenix), Southwest Texas (along the Rio Grande), much of Iowa (numerous small rivers), Southeastern Pennsylvania and New Jersey (Delaware River) and along the Appalachians. The agreement between hazard and flood loss changes is modulated by exposure density and value. For example, although decreased flood depths do not appear in southern California, small decreases actually do, so larger decreases in occurrence loss do appear.

The return period off-plain occurrence loss changes are shown in Figure 12 for the mean GCM view. Again, several return periods are shown to illustrate the insensitivity of the loss change pattern. There is good agreement between the loss changes and the hazard changes shown in Figure 8

. Increases in losses appear across most return periods (even those not shown) where increases in the 100-year RP county average precipitation depth occur. Increases are more widespread for off-plain than for on-plain. The largest contiguous area of increases is actually west of the Rocky Mountains. With few exceptions, counties west of a north-south line from the MT-ID border down to the AZ-NM border show increases. As a state, Colorado shows the largest number of counties (by percent) where decreased losses occur. East of the Rockies, increases and decreases are a random patchwork of results. three other relatively large areas of increase include west Texas/eastern New Mexico, East-central Texas, and a doughnut shaped region centered over Illinois. A notable area of decreased losses appears across the eastern mid-Atlantic

Figure 11

100-YEAR RETURN PERIOD ON-PLAIN OCCURRENCE LOSS CHANGE (%) BY COUNTY AT 25 YEARS (TOP), 50 YEARS (MIDDLE), AND 100 YEARS (BOTTOM).

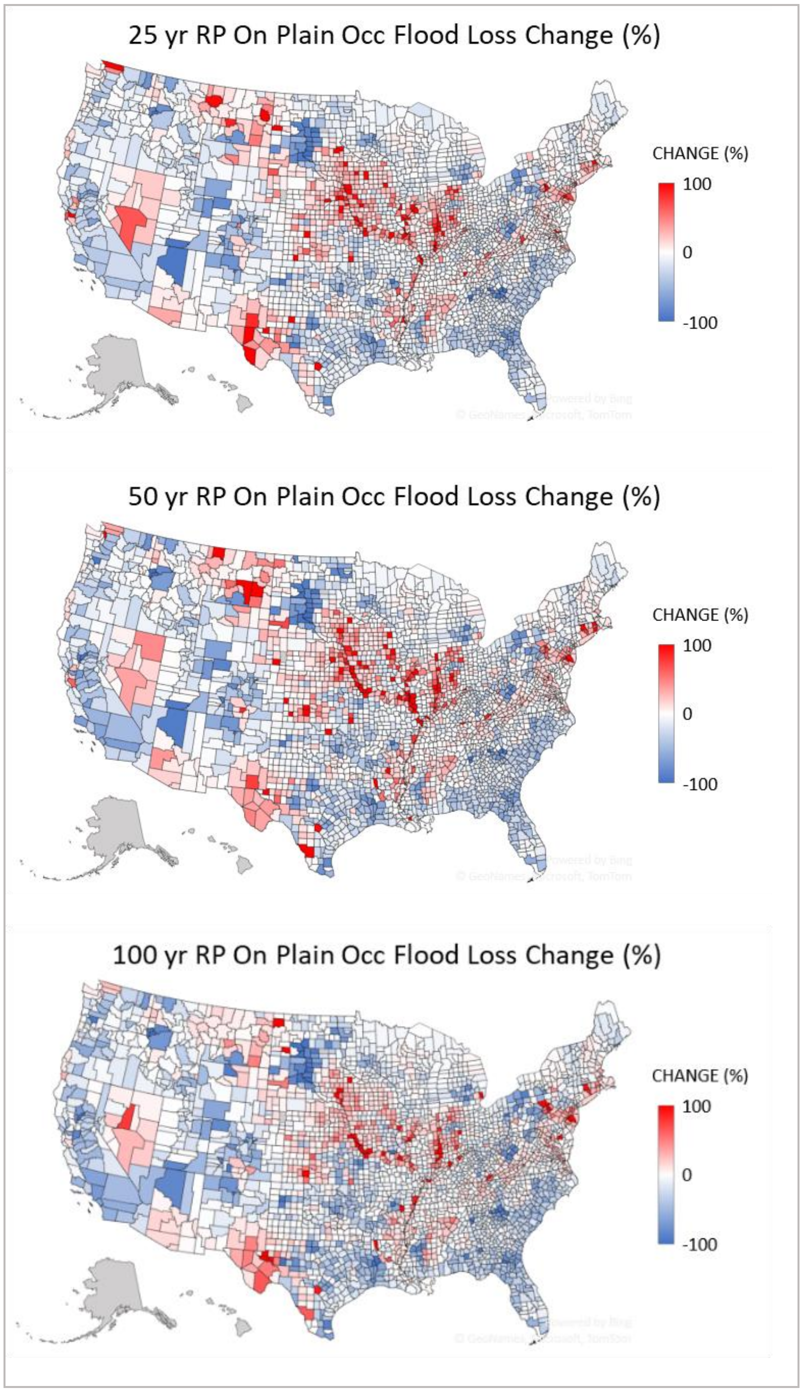

region. This area of decrease may be related to a poleward shift of wintertime storm tracks, which is an expected consequence of climate change (Tamarin and Kaspi 2017). The poleward shift could divert winter storms northward before reaching the mid-Atlantic region.

Figure 12

100-YEAR RETURN PERIOD OFF-PLAIN OCCURRENCE LOSS CHANGE (%) BY COUNTY AT 25 YEARS (TOP), 50 YEARS (MIDDLE), AND 100 YEARS (BOTTOM).

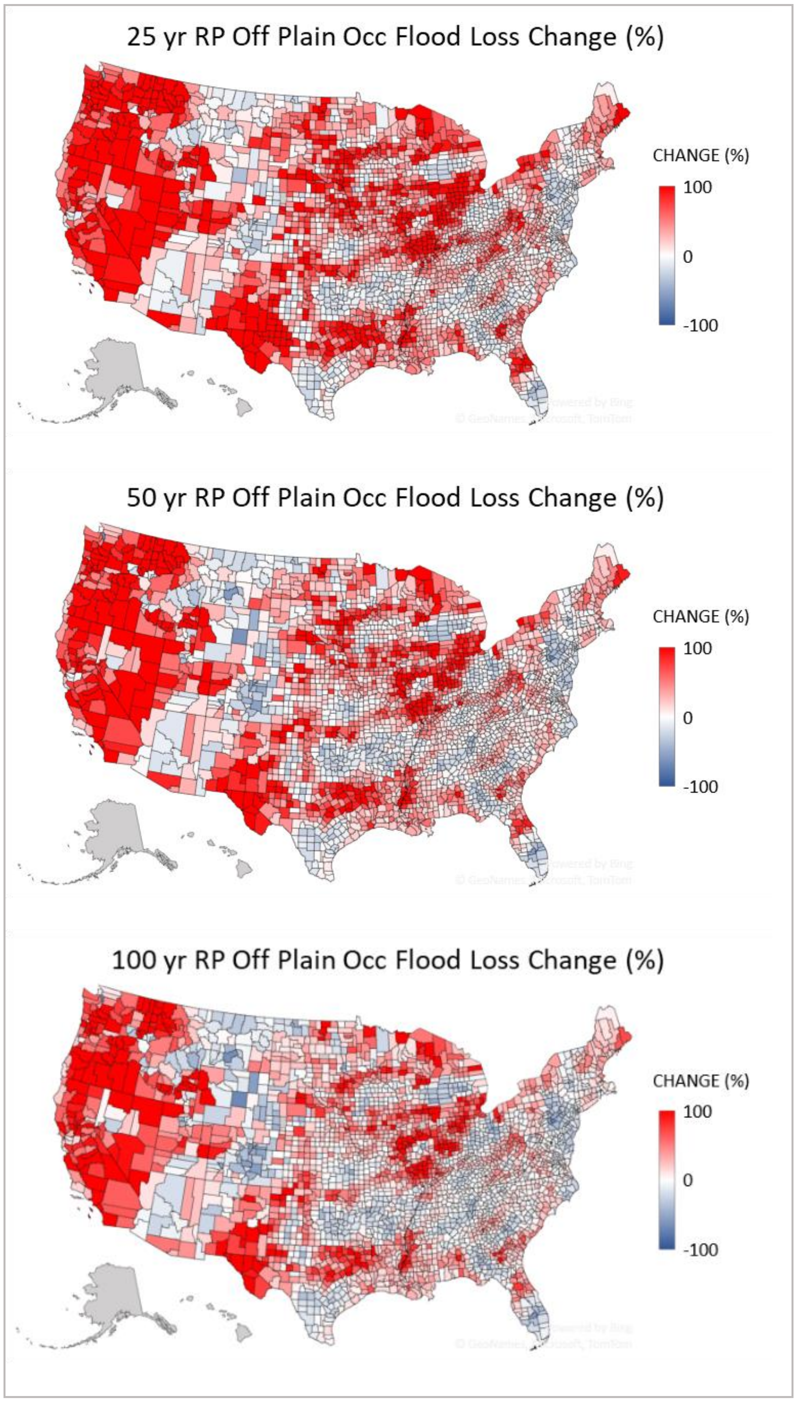

The 2050-2020 changes in annual occurrence losses for on- and off-plain flooding were obtained by estimating the county AOLs for 2020 and 2050 using equation (4) and computing the change relative to 2020. The results are shown in Figure 13 and essentially are smoothed versions (i.e., less abrupt difference in change between adjacent counties) of the return period results.

Without knowing the correlation between on- and off-plain losses for 2050 it is difficult to combine the two results into a single change in AOL for flood by county. However, information about which regions will experience increases in both on- and off-plain flooding is provided in Figure 14. The correlation is determined to a large degree by where on-plain flood losses increase, given that off-plain flood losses increase over a much larger region. Both changes are positive over a large swath in the great plains, oriented Northwest to Southeast – through the Missouri River basin. Narrower swaths with increases in both on- and off-plain flood AOL are located to the east – one along the southern Mississippi River basin and another across the southern Appalachian Region. The area spanned by these swaths as an aggregate suggest increased flood-producing precipitation along a storm track originating in the Pacific Northwest, dipping southward into the southern Plains, and recurving north of the mid-Atlantic region (Tamarin and Kaspi 2017). Smaller regions where on- and off-plain AOL flood losses both show increases west of the Mississippi include the Southwestern part of Texas along the Rio Grande, Nevada, and the coastal Northwest Pacific region. Except for the Pacific Northwest, which is likely related to the enhanced storm track, the correlation is hard to explain without further investigation that is beyond the scope of this study.

Figure 13

AVERAGE OCCURRENCE LOSS CHANGE (%) BY COUNTY FOR ON- (TOP) AND OFF-PLAIN (BOTTOM) FLOODING.

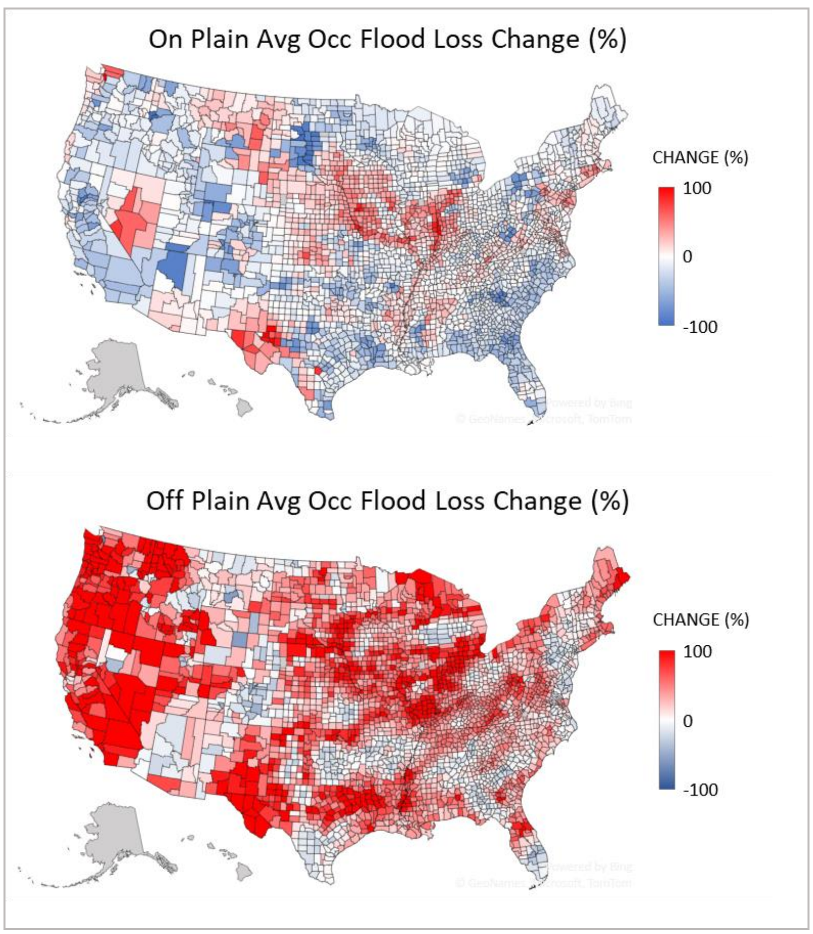

Figure 14
CORRELATION BETWEEN ON- AND OFF-PLAIN AVERAGE ANNUAL OCCURRENCE FLOOD LOSS CHANGES.

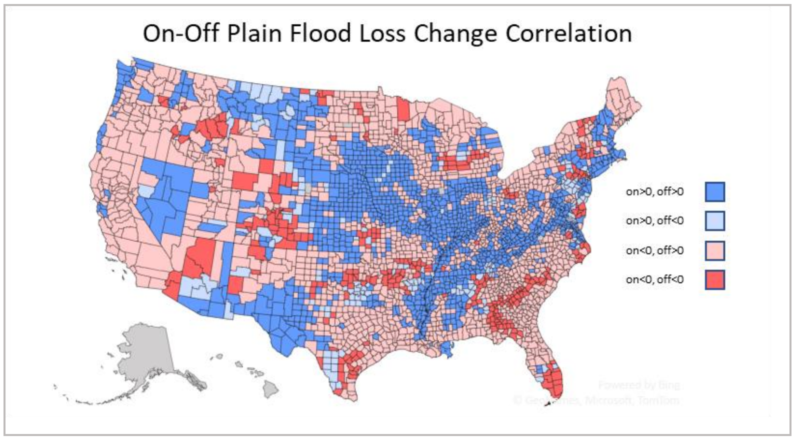

4.2 STATE LEVEL

Analysis at state level for annual occurrence losses (AOL) was accomplished using the method described in 3.2.3.2 State and national losses. Figure 15 shows the result, which is effectively a loss-change-weighted average of the county level loss changes.

Figure 15
STATE-LEVEL ON- AND OFF-PLAIN AVERAGE OCCURRENCE LOSS CHANGES.

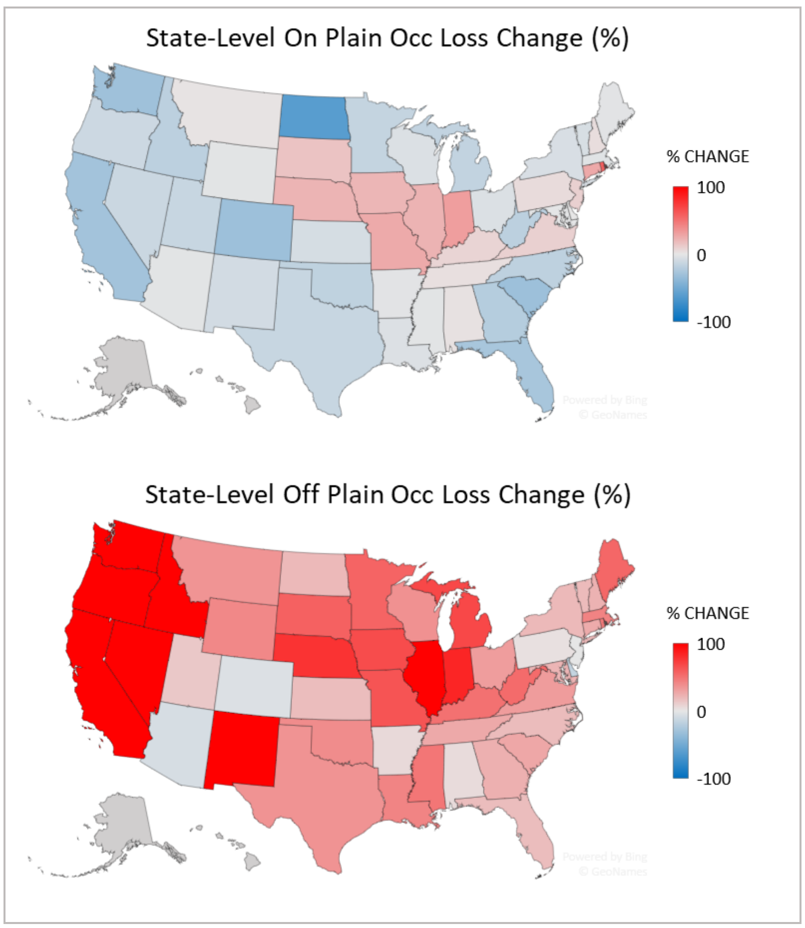

That is, on-plain loss changes (by percent) are mainly negative across the state of South Dakota, but positive changes occur over Sioux Falls in the very Southeastern part of the state, which is the most populous city in South Dakota. Thus, on-plain loss changes are influence by this area to the point where the state, as a whole, exhibits an increase in on-plain flood loss for 2050. For on-plain AOL flood loss changes, no state exceeds 100% increase. For off-plain, several Pacific Northwest States exhibit changes over 100%, with California being the highest at 164%.

4.3 NATIONAL LEVEL

At the national level, defined here as the contiguous U.S., the AOLs from on- and off-plain flooding are projected to change by -6% and +49% by RCP8.5-2050 relative to 2020. Table 3 shows the top five ranking states for on- and off-plain AOL for 2020 and RCP8.5-2050. The top five on-plain loss-causing states in the current climate, accounting for 44% of the sum of state AOLs, are Texas, Louisiana, California, Pennsylvania, and New York. These states, except for Pennsylvania, are projected to have less on-plain loss. By RCP8.5-2050, this ranking changes slightly. Louisiana has the highest because it does not decrease as much as Texas, Pennsylvania has the third highest, and Illinois has the fifth highest since its on-plain AOL increases by 22%.

The top five off-plain loss-causing states is projected to change too. In the current climate, Texas, New York, California, Massachusetts, and New Jersey are the top ranked states. By RCP8.5-2050, California is projected to leapfrog Texas and New York, while Illinois is projected to become the fifth highest, overtaking New Jersey. It is notable that Illinois is projected to become one of the top loss-causing states in both on- and off-plain flood under RCP8.5-2050.

Table 3

TOP FIVE RANKING STATES BY ANNUAL OCCURRENCE LOSS FOR ON- AND OFF-PLAIN FOR 2020 AND RCP8.5-2050

Rank	On-plain 2020	On-plain RCP8.5-2050	Off-plain 2020	Off-plain RCP8.5-2050
1	Texas	Louisiana	Texas	California
2	Louisiana	Texas	New York	Texas
3	California	Pennsylvania	California	New York
4	Pennsylvania	California	Massachusetts	Massachusetts
5	New York	Illinois	New Jersey	Illinois

Off-plain flooding is closely tied to local heavy precipitation events. The increase in overall off-plain loss is due to the increase in maximum daily precipitation in the top loss-causing states. On the other hand, on-plain flooding is determined by other climate variables such as humidity, wind speed and temperature, as well as precipitation. Increases in the rate of evaporation can lead to drier antecedent conditions and lower river levels which can counteract increased precipitation and reduce the on-plain flood risk in the current top loss-causing states.

4.4 UNCERTAINTY

Because the view from the mean GCM does not tell the complete story regarding inter-GCM variability, we show hazard results from all five at the county level and average occurrence loss information at the state level in terms of mean and uncertainty.

The 2020 view of the hazard across the GCMs changes much less so these are not shown. Figure 16 shows changes in the 100-year return period occurrence of county-average flood depth for on-plain flooding along with the mean GCM view for convenience. There are several noteworthy features. One is the apparent lack of consensus in many parts of the U.S. with a few exceptions. One exception is in northern California where all the GCMs show decreased county average flood depth to varying degrees. The mean view therefore is not so much a demonstration of widespread agreement as it is that one or two model results strongly influence the average. The increased county

Figure 16

100-YEAR RETURN PERIOD COUNTY-AVERAGED FLOOD DEPTH DIFFERENCES BETWEEN FUTURE AND CURRENT CLIMATE (2050-2020) FOR ON-PLAIN FLOODING FROM EACH OF THE FIVE GCMS USED IN THE STUDY AS SHOWN IN EACH PANEL AS WELL AS THE MEAN RESULT SHOWN IN THE BOTTOM RIGHT PANEL.

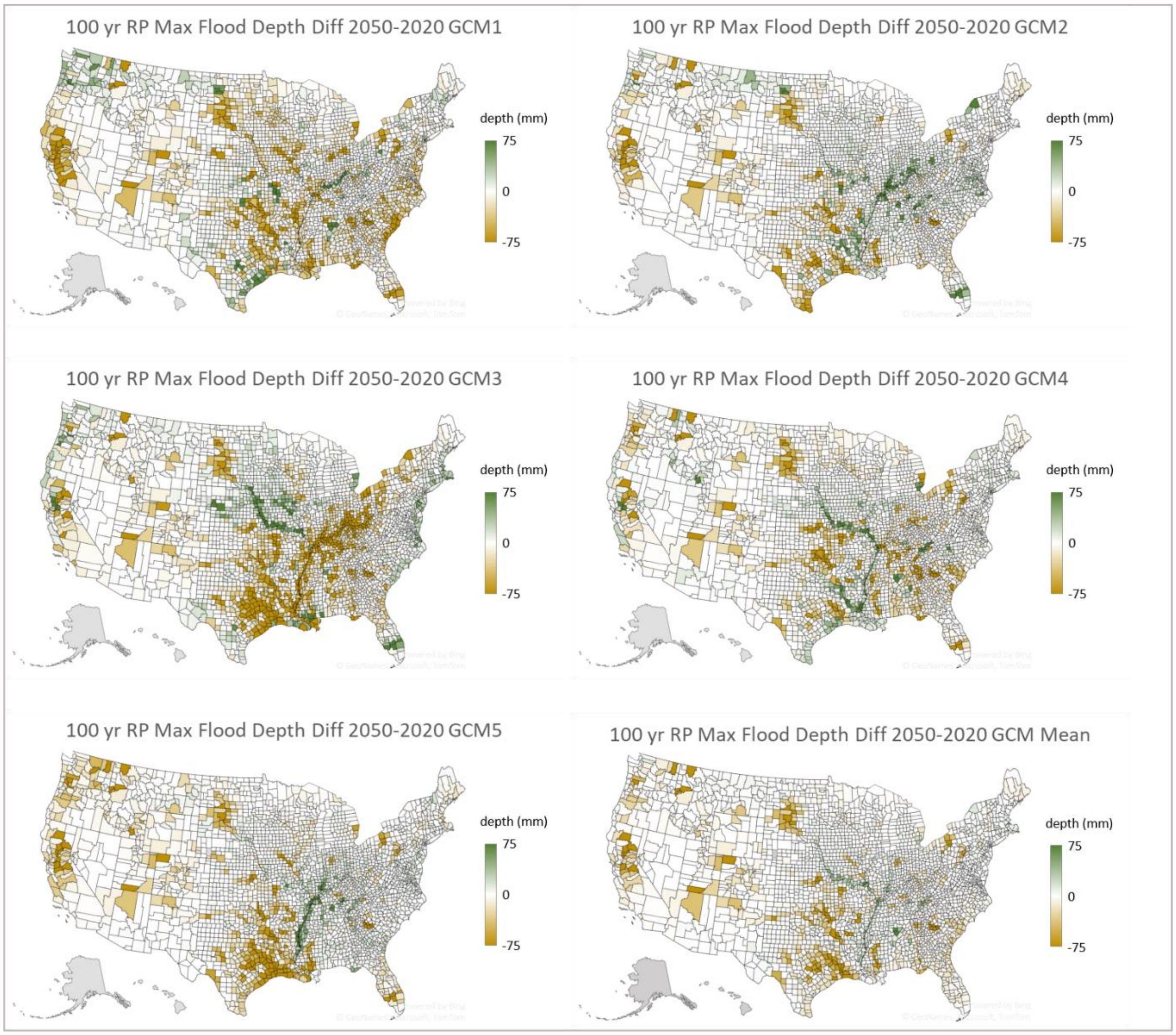

average flood depth along the lower Mississippi River for example seems to be driven by increases from the results in GCM2, GCM4, and GCM5 (mainly) and the increased county-average flood depth along the lower Missouri River is influenced mostly by GCM3 and GCM4. Another is that, perhaps counter to expectations that may be based on results from coarser resolution studies, there is a notable amount of texture in terms of increases and decreases across the country. Also, areas of increase are not nearly as widespread as one might intuitively think. The limited nature of increases in on-plain flooding are physically explainable by the complexity associated with on-plain flooding. Large, prolonged amounts of precipitation in one area may be neutralized by dry antecedent conditions, increased evaporation while water makes its way downstream. However other limitations of the modeling approach may also play a role. The Aqueduct data does not capture small streams and the fact that they may flood more immediately with less impact from how evaporation may influence the result. Although not shown here, other return periods show similar results in terms of the signatures within a GCM and the differences across the GCMs.

Despite off-plain flooding being a more straightforward physical process, there are still differences in the results across the GCMs. Figure 17 shows the 100-year return period occurrence of county-average precipitation depth for the five GCMs along with the mean GCM. Although there is some agreement regionally across some of the models, (e.g., decreased heavy precipitation in eastern VA and NC and FL from GCM3 and GCM4 and increased heavy precipitation across portions of CA in GCM1, GCM2, and GCM4) overall there appears to be low consensus, which is demonstrated by the color shades being overall lighter in the mean GCM view as compared to the result for on-plain flood depth in Figure 16. The behavior within a GCM for other return periods is essentially the same so these are not shown here.

Figure 17

100-YEAR RETURN PERIOD COUNTY-AVERAGED PRECIPITATION DEPTH DIFFERENCES BETWEEN FUTURE AND CURRENT CLIMATE (2050-2020) FOR OFF-PLAIN FLOODING FROM EACH OF THE FIVE GCMS USED IN THE STUDY AS SHOWN IN EACH PANEL AS WELL AS THE MEAN RESULT SHOWN IN THE BOTTOM RIGHT PANEL.

A clearer view of agreement among the GCMs in terms of sign changes is shown in Figure 18. For on-plain flood depths, there is some consensus extending Southeastward from the northern Rockies into the southern Great Plains and along the west side of the Appalachians for increased flood depths (light green to blue colors indicate 3-5 models agree) at the return periods shown although the consensus decreases with increasing return period. There is more consensus for decreased flood depths (yellow to brown colors indicate 3-5 models agree) – in California, the southern Great Plains, and northern Florida. For the on-plain maximum daily precipitation amounts there is in general more agreement among the GCMs that heavy precipitation will increase – in the Pacific Northwest, west Texas, states along the western part of the Gulf of Mexico, portions of the Midwest (Illinois, Indiana, Kentucky, and West Virginia), and northern New England.

Figure 18

DEGREE OF AGREEMENT AMONG THE DIFFERENT GCMS FOR CHANGES IN RETURN PERIOD ON-PLAIN FLOOD DEPTH (LEFT) AND RETURN PERIOD MAXIMUM DAILY PRECIPITATION AMOUNTS (RIGHT). HIGH NUMBERS MEAN MORE AGREEMENT FOR POSITIVE CHANGES. LOW NUMBERS MEAN MORE AGREEMENT FOR NEGATIVE CHANGES.

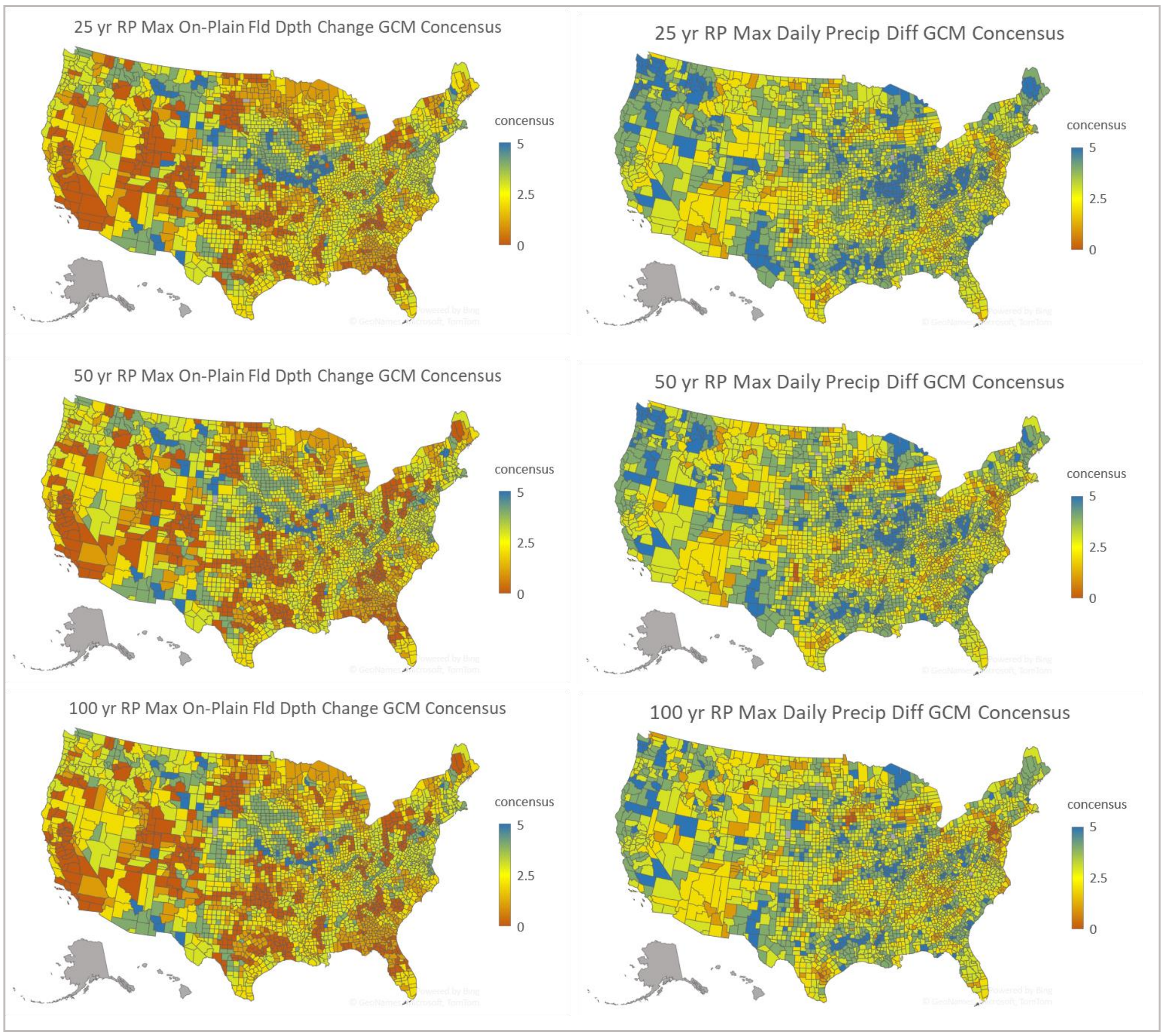

Given the spatial agreement between changes in hazard and changes in loss that are discernible from the mean views described earlier in this section, changes in on- and off-plain occurrence flood losses at the county level can be inferred from changes in the hazard presented in Figure 16 and Figure 17. Impacts at the state level are more complicated, so we present those here. Using the same procedure for determining the state-level AOL from the mean view, county and then state level losses were obtained for each of the five GCMs. Distributions for the spreads were fitted to obtain 5% and 95% confidence intervals at the county- and state-levels. The results are shown in Figure 19. It can be easily seen that the spread in loss change is considerable in both directions although uncertainty in the positive direction is typically larger. Thus, despite the overall (national) negative change in on-plain AOL, it is possible that the on-plain flood AOL could increase at the national level. By the same token, it is possible albeit less so that the off-plain flood AOL could decrease.

Figure 19

SPREAD OF CHANGES IN STATE-LEVEL AOL AND U.S. (RIGHT-MOST BAR) FOR ON-PLAIN FLOOD (UPPER) AND OFF-PLAIN FLOOD (LOWER) BASED ON INFORMATION FROM ALL FIVE GCMS USED. VERTICAL BARS SHOW THE 5-95% CONFIDENCE INTERVAL AND HORIZONTAL LINES INDICATE THE MEAN RESULT.

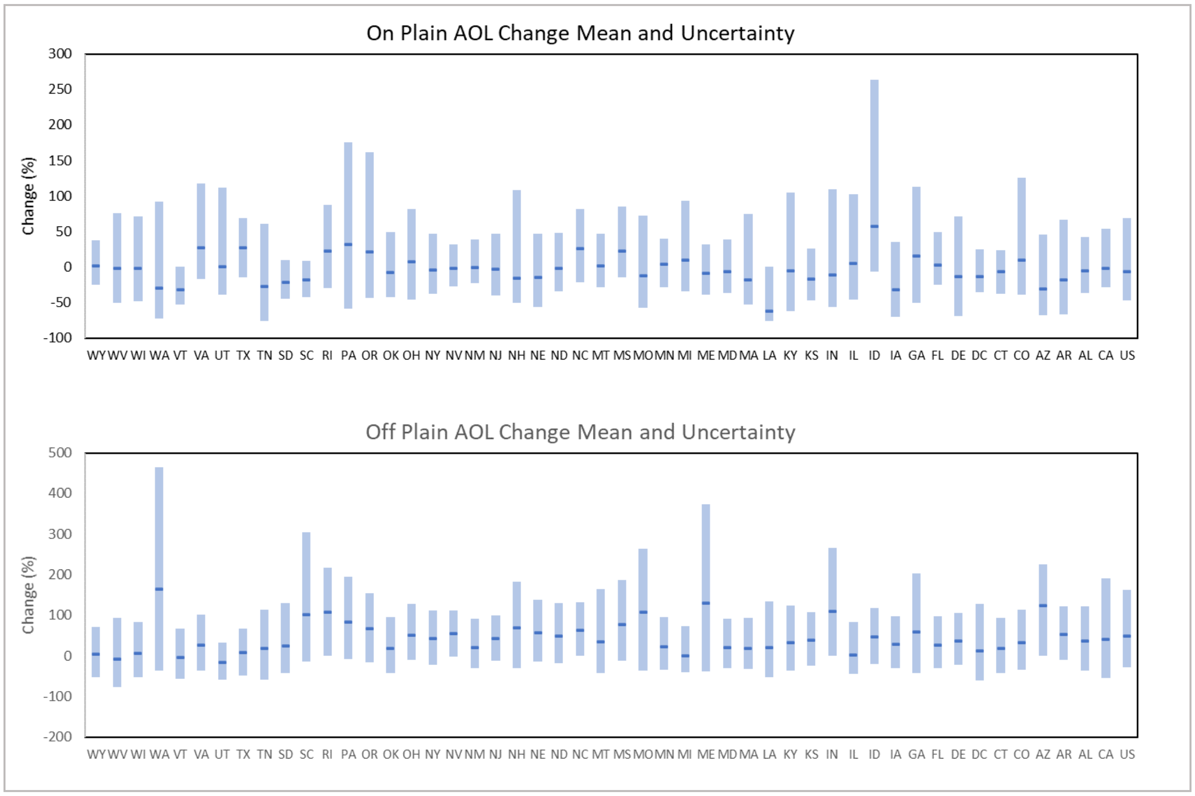

Section 5: Comparison with Wildfire Results

In a companion study for SOA, an analysis of how wildfire risk may change in the future was conducted using the same RCP scenario (8.5) and for the same mid-century time horizon 2050. It was concluded that wildfire loss risk could increase considerably on the order of several tens of percent although there would be regional variability, with the intermountain region of the U.S. likely experiencing the greatest changes percentage wise in annual area burned. However, because that is not where the greatest exposure concentration is that is at risk to wildfire, that is not where the greatest loss changes would occur. We refer the interested reader to that study (Sousounis *et al.* 2021) for more information. Here we compare the results of the wildfire study with those for inland flood.

Figure 20 plots the county AOLs for wildfire in 2020 and RCP8.5-2050 against those for on-plain (A) and off-plain (B) inland flood losses. The current inland flood AOLs are weakly but positively correlated with wildfire AOLs which is largely determined by where exposure is concentrated. The Kendall rank correlation coefficient are given in Table 4. The magnitude of this coefficient should not be compared with a Pearson coefficient. Off-plain AOLs are more strongly correlated to wildfire losses than on-plain AOLs are. This is probably because the county needs to have exposure near a floodplain to experience on-plain losses, while off-plain losses can occur anywhere, even in counties with wildfire fuel.

The correlations weaken from 2020 to RCP 8.5 2050 because while all wildfire county AOLs increase, or stay constant, some inland flood county AOLs decrease. The wildfire AOLs shift to the right of the plots, while the inland flood losses spread up and down.

Figure 21 shows the counties where changes in AOL are positive for wildfire, and off- and on-plain flooding. We can only comment on the western half of the U.S. because that is the current geographical extent of the AIR Wildfire Model for the U.S. The three colors indicate which areas should expect increases from all three (blue); which areas should expect increases from wildfire and either off- or on-plain flooding (green); and which areas should expect increases from just wildfire (yellow). There are no counties where AOL from at least one of these three perils does not increase. The companion wildfire study found that wildfire risk would likely increase everywhere in the domain shown. Most of the map in Figure 21 shows green or blue, which means that many areas should expect increased AOLs from wildfire and flooding. Only portions of Arizona, Colorado, Texas, and Idaho should expect increases in AOL from only wildfire.

Although it is not the case that any one single event will cause significant wildfire and flood loss, there is some utility in considering what the algebraic sum of the AOLs from each of the three perils is and how that quantity may change in the future. we create a multi-peril county-level AOL by summing the AOLs from the individual perils and compare the future climate value to the current climate value. Figure 22 shows the relative impact. Some good news is that regardless of whether all three, only two, or only one risk increases, the increase by county will be under 25% if not negative – for many counties.

Figure 20

COMPARISON OF COUNTY AVERAGE OCCURRENCE LOSS (AOL) FROM WILDFIRE VERSUS ON-PLAIN (A) AND OFF-PLAIN (B) FLOODS FOR 2020 AND RCP8.5-2050.

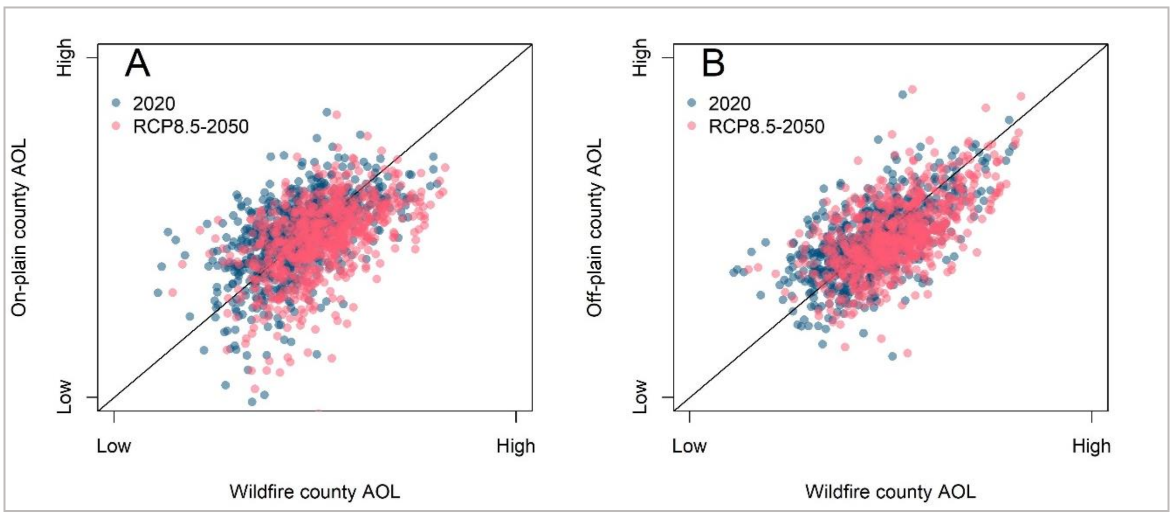

Table 4

KENDALL RANK CORRELATION COEFFICIENTS OF WILDFIRE VERSUS ON- AND OFF-PLAIN COUNTY ANNUAL OCCURRENCE LOSSES FOR 2020 AND RCP8.5-2050.

Flood plain type	Scenario-horizon	Correlation
On-plain	2020	0.42
Off-plain	2020	0.44
On-plain	RCP8.5-2050	0.37
Off-plain	RCP8.5-2050	0.41

Figure 21

MAP SHOWING WHICH COUNTIES FROM THIS AND COMPANION WILDFIRE STUDY SHOULD EXPECT PROJECTED INCREASES IN AOL FROM WILDFIRE, ON- AND OFF-PLAIN FLOODING (BLUE), WILDFIRE AND EITHER ON- OR OFF-PLAIN FLOODING (GREEN), OR ONLY WILDFIRE (YELLOW).

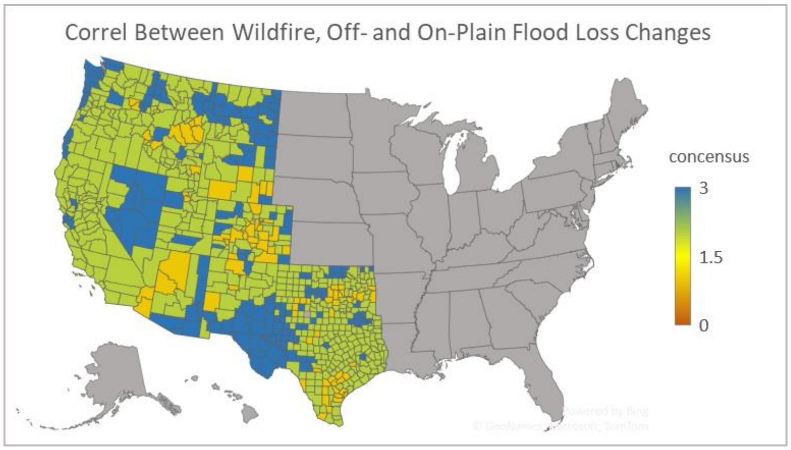

Figure 22

PERCENT CHANGES IN MULTI-PERIL AOL DEFINED BY SUM OF PROJECTED CHANGES IN AOL FROM FUTURE CHANGES IN WILDFIRE RISK, AND ON- AND OFF-PLAIN FLOODING.

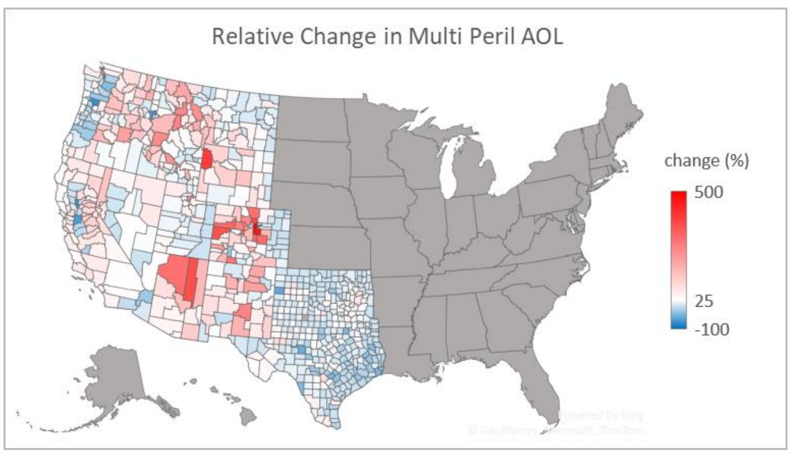

Section 6: Takeaways for Actuaries

Floods have the potential to cause immediate and longer-term elevated risk profiles across many sectors of the economy and health of our society. In the short term, their impact may be more acute and localized. As time passes, these affects may compound and propagate across dimensions, at least in part. Given the findings in this paper, the potential for these risks to grow and the resulting downstream affects should be considered by actuaries across nearly all business practices: Life, Health, Property, and Casualty. The acute affects might be more specific to traditional P&C lines, but the compounding affect should be considered by many that deal with long duration liabilities and assets, which would include both P&C, Life, and in some cases – Health. Therefore, given the nature of this risk, this paper is intended to provide more color to our fundamental understanding of the physical forces at play, which undoubtedly will have impacts on our general society, and more specifically, the actuarial community. Actuaries can use this for their foundational knowledge of the risk and generate a means to test and apply the learnings of this study to our setting of ultimate assumptions. The sensitivities in this paper should also provide the users with a means to understand the uncertainty and the sensitivity of the results to changes in flood frequency and severity.

Climate impacts and changes will not have a uniformed impact across markets, but likely have amplified or depressed impacts in specific locales, product lines, and temporal scales. These impacts may have compounding negative impacts on both the assets and liabilities projections. These risks are likely to affect the general building blocks approach to assumption setting but may also have correlation. Depending on the practice area and the sensitivity of the assets and liabilities, the negative and dual effect on liabilities and assets may prove challenging to mitigate. Therefore, we suggest thinking of the risk in three dimensions – general impact to risks, specific / localized impact, and trend changes between now and 2050. For some actuarial practices, it may be hard to implement spatial correlations, while others may be challenged by the temporal risk assessment.

Across the board, there are numerous means to model this risk and actuaries should become more familiar with traditional models in other actuarial practice areas or with using other experts outside of their traditional domain. We encourage actuaries when using outside models to apply them within the framework and in the spirit of ASOP 38 – Using Models Outside the Actuary's Expertise. Though ASOP 38 has been more traditionally associated with P&C, we believe there are great learnings to be had from the life and health space, especially as it has to do with modeling the impacts of flood on the given practice areas of the life, health community, investment, and other. We also encourage the use of ASOP 56 – Modeling to help frame the development of these models.

6.1 RISK ASSESSMENT

We anticipate the first means to understanding the risk may be to start quantifying it at a high level before we start to develop large scale systems. As such, we propose using our discussions in this paper to help frame the approximate rules of thumb.

When construction more complex systems, the risk is probably best thought of using the traditional topics and material covered of Construction of Actuarial Models. Most specifically, via a frequency and severity. For the non-one-year assessment, there is the added complexity of correlated trend risk which would influence the set of distributions. This can be done using a step process and each step equates to some time interval, or alternatively, this could be done in one continuous system.

This risk will clearly vary by policy and temporal period assessed. Therefore, we have provided the information below as food for thought as you think through this risk relative to actuarial practice area. This list is not intended to be exhaustive in either its breath across the actuarial departments, nor in the commentary around any given practice area. Please use this for contextual purposes only.

6.1.1 PROPERTY INSURANCE

Probably the most obvious would be the impact to direct loss to buildings, their contents, and time element. The complexity would likely be similar to traditional catastrophic risk modeling. Still challenging, though less esoteric for the life and health space and likely more current and applicable data to derive the risk impact from. The downside for this risk is the extreme nature it may occur each year, standing the chance to cause ruin. Though the risk may accumulate over time, each year is substantively independent of the prior and firms have the ability to modify premiums on a per-annum basis. Thus, substantively mitigating the ultimate nature of the ultimate risk.

6.1.2 LIFE, HEALTH, AND WORKER'S COMPENSATION

This one may be the most complex. The number of people whose health is affected indirectly from floods (e.g., from mosquito borne illness, contaminated drinking water, respiratory illness from mold growth) is much harder to identify. Additionally, changes in short temporal timescales, likely will be a poor gauge to the ultimate risk –

analogous to ultimate trend risk vs recent history. Additionally, developing retrospective models will almost certainly underestimate the risk as the historical record is not likely to contain the appropriate scale. Therefore, we suggest development of a prospective probabilistic methods to derive "best estimates" and uncertainty around that estimate.

One means to derive comparable risk assessment is to look at appropriate metrics for all flood impacted aspects of health by various geographies to understand the illness severity. Combining this with a forward trend model will allow firms to gage the localized impact at various time intervals. This may be further complicated by the effects of technological advancements, both in the form of medical and flood mitigation efforts. Fortunately, the process is modellable (though complex) and trackable (Kramer *et al.*, 2019).

Current underwriting and risk measurement practices are not well suited for understanding, accounting, or easing the affects that may arise. Mortality projections are, in general, based on historical experience. This event is non-existent in the historical record. Even if it was captured well, the localized impact for areas would be substantively different. Additional, and for good reason, localized mortality assessments are not often permitted.

Section 7: Closing Remarks

This study uses available downscaled output from five different GCMs as part of the Coupled Model Intercomparison Project Phase 5 (CMIP5) and information from the AIR Inland Flood and Hurricane Models for the U.S. to evaluate how changes in flooding will impact insurable losses in the future. On-plain annual occurrence maps for nine different return periods at 1 km resolution are sourced from Aqueduct Floods. Three extra return periods are created, and the maps are aggregated to the county-level. Daily precipitation at 4 km resolution, downscaled from the same five GCMs, is used to obtain county-level annual occurrence maps for the same twelve return periods. Coastal flooding is not addressed in this study.

This study does not account for changes that may occur to infrastructure or land use, or management practices that may affect the severity or frequency of floods. It also does not account for changes in exposure or building codes that could influence the insurable losses from flood. Thus, the results of the study may be interpreted as a flood sensitivity study, where the only impact to flood loss is from climate change. That said, there are a host of different types of uncertainty, and the readers should be aware of them as they use information from this study for any decision making. We describe them below, but they are not in any particular order, given that further study would be needed to quantify the relative impacts from each type.

One type of uncertainty that was addressed in some detail is that from the range of hydrological possibilities from the five GCMs used, which propagates to the loss results. As was shown in the previous section, the spread is considerable although some larger scale areas of agreement do exist for areas that may see increased on-plain flood depths and loss, and areas that would experience heavier precipitation and off-plain flood loss as separate results, and both together. The spread in the GCM results demonstrates the importance for not making decisions based solely on mean results. It is also important to understand that the uncertainty and the mean values analyzed and obtained for this study are based on a subset of GCMs that are part of suite of CMIP5 models although as shown recently by Hirabayashi (2021) the results from the subset used in this study generally agree with those obtained from a larger set. That study also included a comparison to results using CMIP6, which do show some changes relative to the CMIP5 results although the big picture of increased flooding over the central and Southeastern U.S. and less flooding in the west remains the same. The similarities between CMIP5 and CMIP6 are also explained in the latest report (AR6) from the Intergovernmental Panel on Climate Change (IPCC 2021).

Another type of uncertainty is associated with the RCP scenarios themselves. It is important to recognize that these scenarios are not forecasts per se and because of that, it is not appropriate to assign probabilities to them – at least not preferentially. From that standpoint they are all equally probable. Although the RCP 8.5 scenario is on the high end of the group of 4 RCP scenarios (RCP 2.6 reflects the smallest impact from climate change because of assumed changes in emissions) it is a scenario that society have been following over the last 15 years. Related to the uncertainty of the RCP scenario is the spread of climate change within a particular RCP scenario. For example, an RCP 8.5 is expected to yield a ~2.0 ^{o}C temperature increase +/- 0.5 ^{o}C by 2050. To some extent, the selection of several GCMs that were all forced under an RCP 8.5 scenario accounts for this aspect.

There is also uncertainty in the results that was imposed because of the methodology we used. For example, return periods values for low-probability events were estimated using only several decades worth of output from the GCMs and Extreme Value Theory. And, although many of the exhibits shown in this report focus on relatively low return periods (<= 100 years), the information at higher return periods affects the calculation of AOLs. Another type uncertainty introduced by the methodology for off-plain flooding especially stems from the use of return period precipitation values as a proxy for flooding. However, because the hazard metric (precipitation depth) is combined with loss information from the AIR Models, to create damage functions from the perspective of the hazard metric used makes this limitation less impactful. Related to this approach is the assumption that an x-year RP hazard metric results in an x-year RP loss, which is not a bad assumption at a small scale (e.g., county-level). Without further study and analysis, it is difficult to quantify these methodology-based uncertainties.

As noted earlier at the beginning of this section, the focus was on impacts on loss to U.S. insurable property from climate change. Assumptions about how flood defenses, infrastructure, and building codes and even land-use and land-cover will change in the future are omitted. But these will likely change, which is hopefully the case, based on studies like this one. Thus, there should be no expectation that in the year 2050, an analysis of flood risk for what will be the current climate at that time, will agree with the results in this study. Instead, by providing estimates of the cost of not mitigating greenhouse gas emissions and not adapting to increased flood risk, this study can be used to estimate the savings made by transitioning to a greener economy and improving urban drainage capacities and flood defenses in specific areas of the U.S.

Finally, we emphasize the uncertainty with interpreting results at very small scale. Although GCM output for this study was available at one-to- four-kilometer resolution, because of all the uncertainties already described, there is a danger in over-emphasizing the results at such small scales and to a lesser degree even county-level. That is the primary reason for upscaling our results to state and national levels, where more confidence, stemming from more widespread agreement in the GCMs exists.

In closing, it is important to emphasize that despite the uncertainties and limitations, the study provides useful guidance for how climate change likely will affect U.S. flood risk in the future. As disturbing as some of the changes are – particularly for off-plain flooding and particularly for west coast states, we note that at least from a hazard perspective, we have agreement with results from other recent studies using different methods from different researchers based on different data. And, especially with what a potentially damaging future may bring, it is better to have quantitative information on what the changes in hazard mean for U.S. flood losses now, in order to give time to react and protect against the projected losses.

Section 8: Acknowledgments

The researchers wish to extend their gratitude to the POG members and SOA members for their guidance throughout the project and for their careful review of this report.

Project Oversight Group members:

Joan Barrett, FSA, MAAA; Consultant, Axene Health Partners

Laura Bass, FSA, MAAA;

Sam Gutterman, FSA, MAAA, FCAS, FCA, HONFIA, CERA; Director, PricewaterhouseCoopers

Steve Kolk, ACAS, MAAA; Climate Data Scientist, Kolkulations LLC

Julie Meadows, FSA, MAAA, CERA; Associate Director, Actuarial Services at UnitedHealth Group

Shone Mousseiri, ASA, ACIA, PRM, GradStat; Analyst, Manulife

Brad Paulis, ASA, MAAA, FCA; Partner, Continuing Care Actuaries

Didier Serre, FSA; Head of Climate Risk Modeling and Research; Clearsum

Manyu Wong, FSA, CERA; Business Steering Specialist, Vice President, Swiss Re

Cathy (Cici) Zhang, FSA, MAAA; Consulting Actuary, Milliman

At the Society of Actuaries:

Rob Montgomery, ASA, MAAA; Independent Consultant, Project Manager

Erika Schulty, Research Associate, Society of Actuaries

Appendix A: Map of Major U.S. Rivers

Figure 23

MAP OF THE CONTIGUOUS UNITED STATES SHOWING THE STATES AND MAJOR RIVERS.

References

Abatzoglou, J. T., 2011: Development of gridded surface meteorological data for ecological applications and modelling. *Int. J. Climatol.*, **31**, 121–131.

Abatzoglou, J. T. and T. J. Brown, 2012: A comparison of statistical downscaling methods suited for wildfire applications. *Int. J. Climatol*., **32**, 772-780, https://doi.org/10.1002/joc.2312.

Alfieri, L., B. Bisselink, F. Dottori, G. Naumann, A. de Roo, P. Salamon, K. Wyser, and L. Feyen, 2017: Global projections of river flood risk in a warmer world. *Earth's Future*, **5**, 171-182, https://doi.org/10.1002/2016EF000485

Anderson, B. T., D. J. Gianotti, and G. D. Salvucci, 2015: Detectability of historical trends in station-based precipitation characteristics over the continental United States. *J. Geophys. Res. Atmos.*, **120**, 4842–4859, doi:10.1002/2014JD022960.

Arnell, N. W., B. Lloyd-Hughes, 2014: The global-scale impacts of climate change on water resources and flooding under new climate and socio-economic scenarios. *Climatic Change,* **122,** 127–140, https://doi.org/10.1007/s10584-013-0948-4.

Easterling, D. R., K. E. Kunkel, M. F. Wehner, and L. Sun, 2016: Detection and attribution of climate extremes in the observed record. *Weather and Climate Extremes*, **11**, 17–27, doi:10.1016/j.wace.2016.01.001.

FEMA, 2007: Floodplain Management: Principles and Current Practices, An Academic and Emergency Management Training Program. Avail. On-line: FEMA Higher Education Program | AEMRC – Floodplain Management: Principles and Current Practices.

First Street Foundation. First Street Foundation Technical Documentation. 2020. Available online: https://assets.firststreet.org/uploads/2020/06/FSF_Flood_Model_Technical_Documentation.pdf.

First Street Foundation. The First National Flood Risk Assessment: Defining America's Growing Risk. 2020. Available online: https://assets.firststreet.org/uploads/2020/06/first_street_foundation__first_national_flood_risk_assessment.pdf.

Florida Commission on Hurricane Loss Projection Methodology, 2021: Modeler Submission, Current Year Hurricane Model Submissions, Available online: https://www.sbafla.com/methodology/ModelerSubmissions/CurrentYearHurricaneModelSubmissions.aspx

Hirabayashi, Y., M. Tanoue, O. Sasaki, *et al.,* 2021*:* Global exposure to flooding from the new CMIP6 climate model projections. *Sci. Rep.,* **11,** 3740, https://doi.org/10.1038/s41598-021-83279-w

Janssen, E., R. L. Sriver, D. J. Wuebbles, and K. E. Kunkel, 2016: Seasonal and regional variations in extreme precipitation event frequency using CMIP5. *Geophys. Res. Lett.*, **43**, 5385–5393, doi:10.1002/2016GL069151.

Koirala, S.; Y. Hirabayashi, R. Mahendran, K. Shinjiro, 2014: Global assessment of agreement among streamflow projections using CMIP5 model outputs. *Environ. Res. Lett.*, **9(6)**, 1-11, DOI:10.1088/1748-9326/9/6/064017

Kraemer, M.U.G., Reiner, R.C., Brady, O.J. *et al.*, 2019: Past and future spread of the arbovirus vectors Aedes aegypti and Aedes albopictus. *Nat. Microbiol*., **4**, 854–863, https://doi.org/10.1038/s41564-019-0376-y

Kunkel, K. E., D. R. Easterling, D. A. Kristovich, B. Gleason, L. Stoecker, and R. Smith, 2012: Meteorological causes of the secular variations in observed extreme precipitation events for the conterminous United States. *J. Hydrometeor.*, **13**, 1131–1141, doi:10.1175/JHM-D-11-0108.1.

Kunkel, K. E., D. R. Easterling, D. A. R. Kristovich, B. Gleason, L. Stoecker, and R. Smith, 2010: Recent increases in U.S. heavy precipitation associated with tropical cyclones. *Geophys. Res. Lett.*, **37**, L24706, doi:10.1029/2010GL045164.

Myhre, G., K. Alterskjær, C.W. Stjern, *et al.,* 2019: Frequency of extreme precipitation increases extensively with event rareness under global warming. *Sci. Rep.* **9,** 16063, https://doi.org/10.1038/s41598-019-52277-4

National Hurricane Center, 2021: North Atlantic Storm Database, HURDAT2: Atlantic Tracks File 1851-2007, Atlantic Oceanographic and Meteorological Laboratory, Hurricane Research Division. Available at http://www.nhc.noaa.gov/pastall.shtml.

Pall, P. C. M. P., M. F. Wehner, D. A. Stone, C. J. Paciorek, and W. D. Collins, 2017: Diagnosing anthropogenic contributions to heavy Colorado rainfall in September 2013. *Weather and Climate Extremes*, **17**, 1–6, doi:10.1016/j.wace.2017.03.004.

Prein, A. F., R. M. Rasmussen, K. Ikeda, C. Liu, M. P. Clark, and G. J. Holland, 2017: The future intensification of hourly precipitation extremes. *Nature Climate Change*, **7**, 48–52, doi:10.1038/nclimate3168.

Sousounis, P., A. Clarke, and D. Fulham, 2021: Potential Impacts of Climate Change on U.S. Wildfire Risk by Mid Century, *SOA Research Institute Report*, 48 pp. avail. at: https://www.soa.org/resources/research-reports/2021/climate-change-impacts-to-us-wildfire-risk/

Sutanudjaja, E. H., R. van Beek, N. Wanders, Y. Wada, J. H. C. Bosmans, N. Drost, R. J. van der Ent, I. E. M. de Graaf, J. M. Hoch, K. de Jong, D. Karssenberg, P. López López, S. Peßenteiner, O. Schmitz, M. W. Straatsma, E. Vannametee, D. Wisser, and M. F. P. Bierkens, 2018: PCR-GLOBWB 2: a 5 arcmin global hydrological and water resources model, *Geosci. Model Dev.*, **11**, 2429–2453, https://doi.org/10.5194/gmd-11-2429-2018, 2018.

Tamarin, T., and Y. Kaspi, 2017: The poleward shift of storm tracks under global warming: A Lagrangian perspective, *Geophys. Res. Lett.*, **44**, 10,666– 10,674, doi:10.1002/2017GL073633.

Taylor, K. E., R. J. Stouffer, G. A. Meehl, 2012: An Overview of CMIP5 and the experiment design. *Bull. Amer. Meteor. Soc.,* **93**, 485-498.

Ward, P.J., B. Jongman, F. S. Weiland, A. Bouwman, R. van Beek, M. F. P. Bierkens, W. Ligtvoet, and H. C. Winsemius, 2013: Assessing Flood Risk at the Global Scale: Model Setup, Results, and Sensitivity. Environ. Res. Lett., 8: 044019, https://doi.org/10.1088/1748-9326/8/4/044019 .

Ward, P. J., H. C. Winsemius, S. Kuzma, M. F. P. Bierkens, A. Bouwman, H. de Moel, A. Díaz Loaiza, *et al.*, 2020: Aqueduct Floods Methodology. Technical Note. Washington, D.C.: World Resources Institute. Available online at: www.wri.org/publication/aqueduct-floods-methodology.

Westra, S., L. V. Alexander, and F. W. Zwiers, 2013: Global increasing trends in annual maximum daily precipitation. *J. Climate*, **26**, 3904–3918, doi:10.1175/JCLI-D-12-00502.1.

Winsemius, H. C., L. P. H. van Beek, B. Jongman, P. J. Ward, and A. Bouwman, 2013: A Framework for Global River Flood Risk Assessments. *Hydr. Earth Sys. Sci.*, **17**, 1871–92, https://doi.org/10.5194/hess-17-1871-2013 .

Wobus, C., E. Gutmann, R. Jones, M. Rissing, N. Mizukami, M. Lorie, H. Mahoney, A. W. Wood, D. Mills, and J. Martinich, 2017: Climate change impacts on flood risk and asset damages within mapped 100-year floodplains of the contiguous United States, *Nat. Hazards Earth Sys. Sci.*, **17**, 2199–2211, https://doi.org/10.5194/nhess-17-2199-2017 .

Yamazaki D., S. Kanae, H. Kim, and T. Oki, 2011: A physically based description of floodplain inundation dynamics in a global river routing model. *Water Resour. Res.*, **47**, W04501.

Feedback

About The Society of Actuaries Research Institute

Serving as the research arm of the Society of Actuaries (SOA), the SOA Research Institute provides objective, data-driven research bringing together tried and true practices and future-focused approaches to address societal challenges and your business needs. The Institute provides trusted knowledge, extensive experience and new technologies to help effectively identify, predict and manage risks.

Representing the thousands of actuaries who help conduct critical research, the SOA Research Institute provides clarity and solutions on risks and societal challenges. The Institute actuaries, academics, employers, the insurance industry, regulators, research partners, foundations and research institutions, sponsors and non-governmental organizations, building an effective network which provides support, knowledge and expertise regarding the management of risk to benefit the industry and the public.

Managed by experienced actuaries and research experts from a broad range of industries, the SOA Research Institute creates, funds, develops and distributes research to elevate actuaries as leaders in measuring and managing risk. These efforts include studies, essay collections, webcasts, research papers, survey reports, and original research on topics impacting society.

Harnessing its peer-reviewed research, leading-edge technologies, new data tools and innovative practices, the Institute seeks to understand the underlying causes of risk and the possible outcomes. The Institute develops objective research spanning a variety of topics with its strategic research programs: aging and retirement; actuarial innovation and technology; mortality and longevity; diversity, equity and inclusion; health care cost trends; and catastrophe and climate risk. The Institute has a large volume of topical research available, including an expanding collection of international and market-specific research, experience studies, models and timely research.

Society of Actuaries Research Institute
475 N. Martingale Road, Suite 600
Schaumburg, Illinois 60173
www.SOA.org